University of Bergen
University of Brescia
CERN, Geneva
University of Genova
Heidelberg University
Max Planck Institute for Nuclear Physics, Heidelberg
University of Trento
University of Lyon
University of Milano
Politecnico di Milano
Institute of Nuclear Research of the Russian Academy of Science, Moscow
University of Oslo
Lab. Aime' Cotton Orsay
University of Pavia
Czech Technical University, Prague
INFN Sections of Genova, Milano, Padova, Pavia, Trento
Stefan Meyer Institute, Vienna

Antihydrogen formation via charge exchange between positronium and antiproton

Nicola Zurlo [University of Brescia & INFN Pavia]
on behalf of the AEgIS Collaboration

zurlo@cern.ch

AEgIS (Antimatter Experiment Gravity Intereferometry Spectroscopy) goals

Test the validity of fundamental principles with antihydrogen : WEP – CPT

g measurement on anti-H:
vertical shift of a cold beam travelling through a grating system coupled with a position sensitive detector (classical deflectometer or interferometer)

Proof of principle of tiny vertical force measurement with the grating system with pbars in
Nature Comm. 5, 4538 (2014) AEgIS Coll,
“A moiré deflectometer for antimatter”

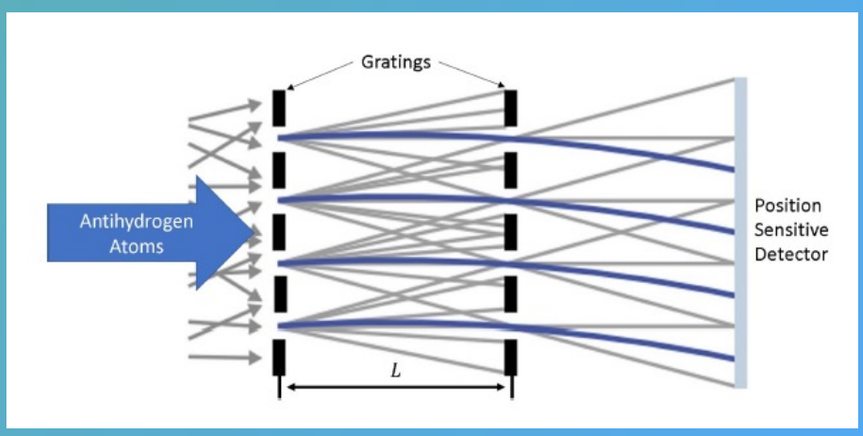

AEgIS Methods

- produce pulsed antihydrogen beam
- Antihydrogen formation through $\overline{p} + Ps^* \rightarrow \overline{H}^* + e^-$
- Ps formation via impact of e+ on converter material
- Ps laser excitation to Rydberg states
- Ps* interaction with pbar previously stored close to the target
- Hbar formation in Rydberg states
- Beam formation: Hbar acceleration with suitable electric fields

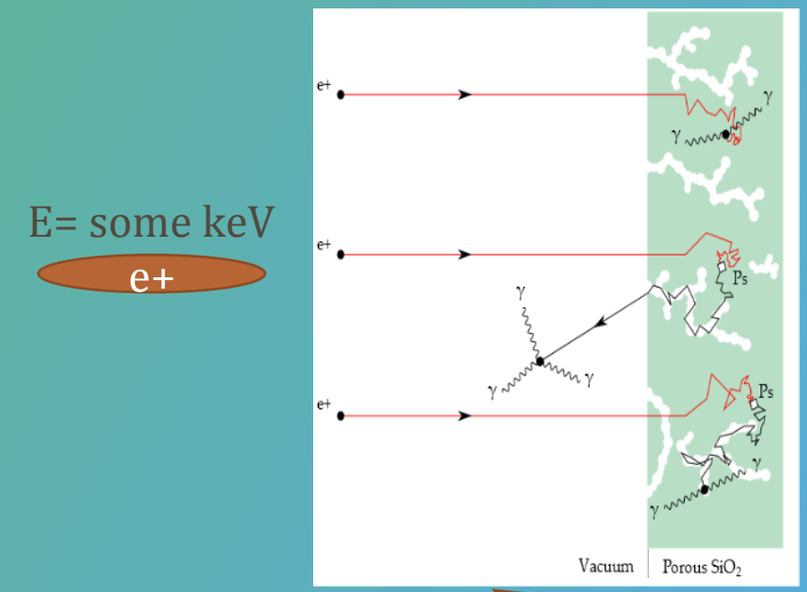

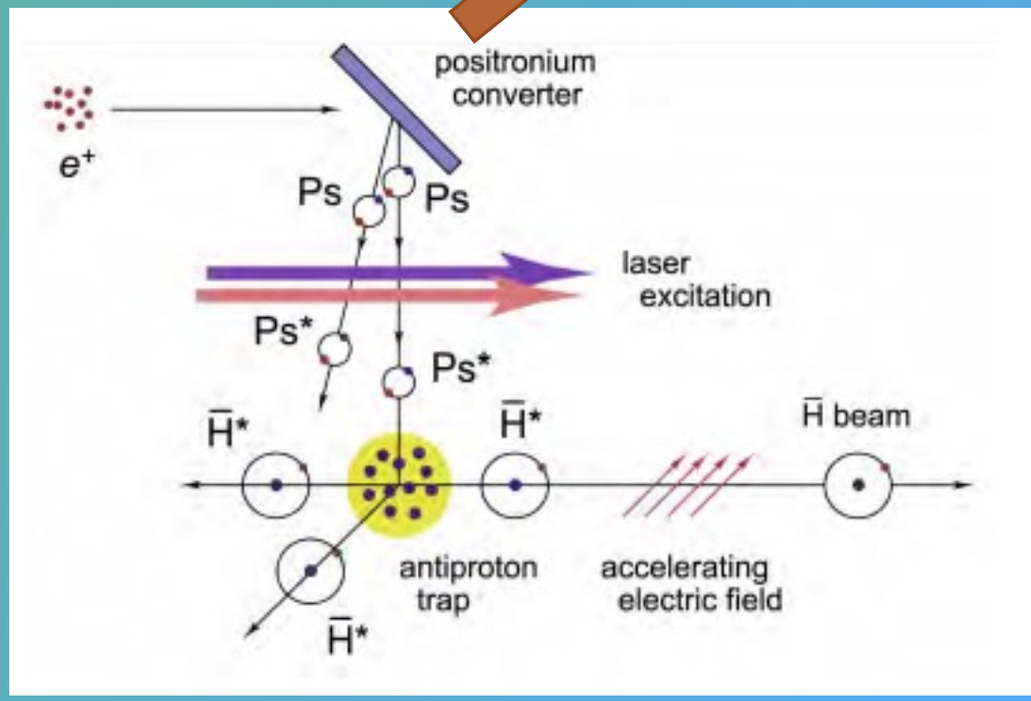

AEgIS Apparatus

- Accumulator for e+
- Magnetic transfer line for e+
- Superconducting magnetic fields (5T, 1T)
- Cryogenic traps (105 electrodes)
- antiH detector (scintillating fibers)
- External plastic scintillators
- Internal (MCP+phosphor screen & Faraday cups in cryogenic UHV)
- lasers
- Additional detectors
- POSITRON MEASUREMENT setup

Ps test setup
used for measurements with Ps (excitation etc.)

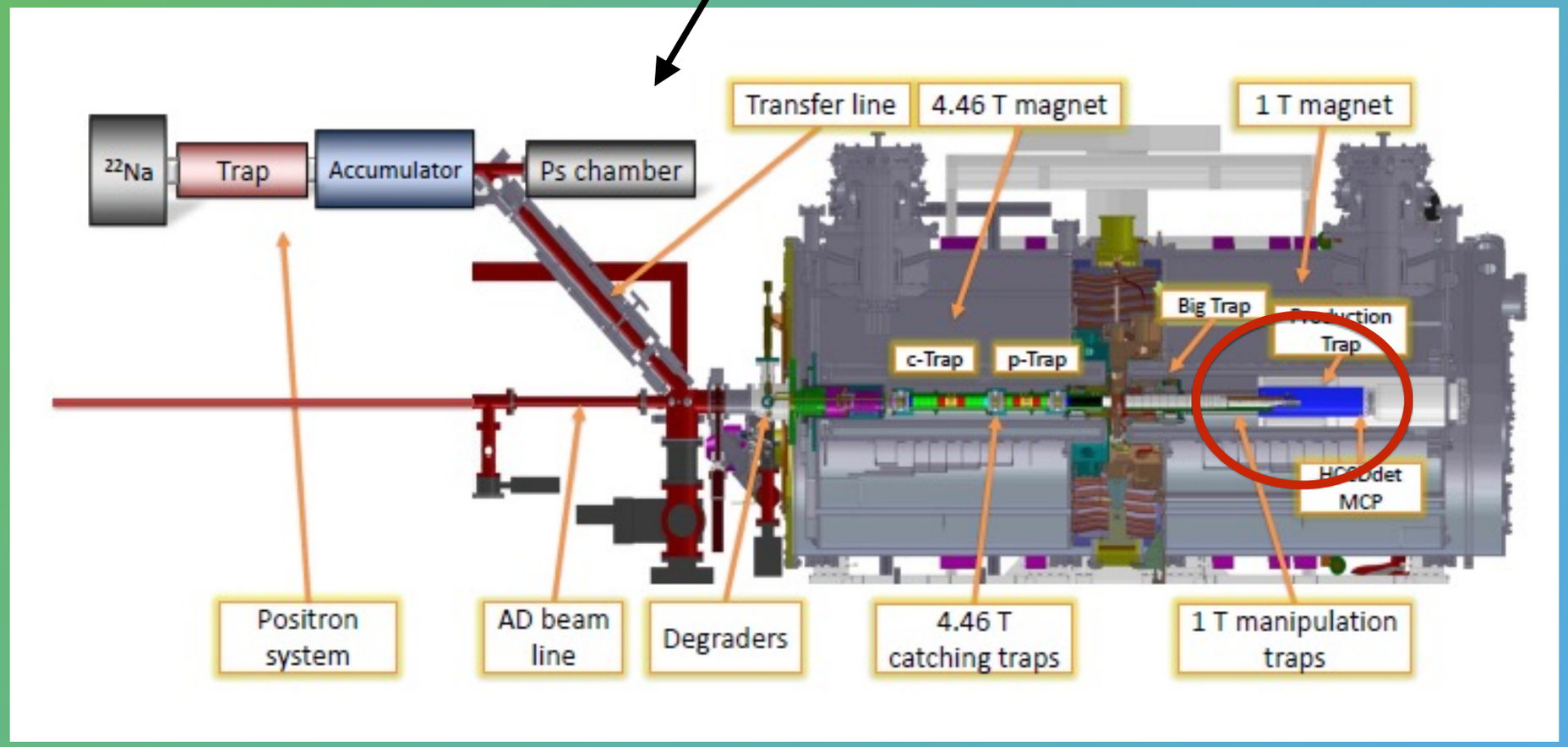

see Daniel Krasnicky's yesterday talk

AEgIS Method

Capture of antiprotons from the CERN-AD
Cooling of the trapped antiprotons

Positronium (e^+e^-) production by e^+ on SiO_2
Ps laser excitation to Rydberg state

Interaction of Ps* with the antiproton cloud

$$\overline{p} + (Ps)^* \rightarrow \overline{H}^* + e^-$$

Positronium charge exchange reaction

First proposed by B.I. Deutch et al., Proceedings of The First Workshop on Antimatter Physics at Low Energy, 371 (1986).

same charge exchange reaction with a similar technique based on Rydberg cesium performed by ATRAP: C. Storry et al., Phys. Rev. Lett. 93 (2004)

ADVANTAGES
- Large cross section $\sigma \propto (n_{Ps})^4$
- Narrow and well defined band of final states ($n_{\bar{H}} \approx \sqrt{2n_{Ps}}$, with a rms of few units)

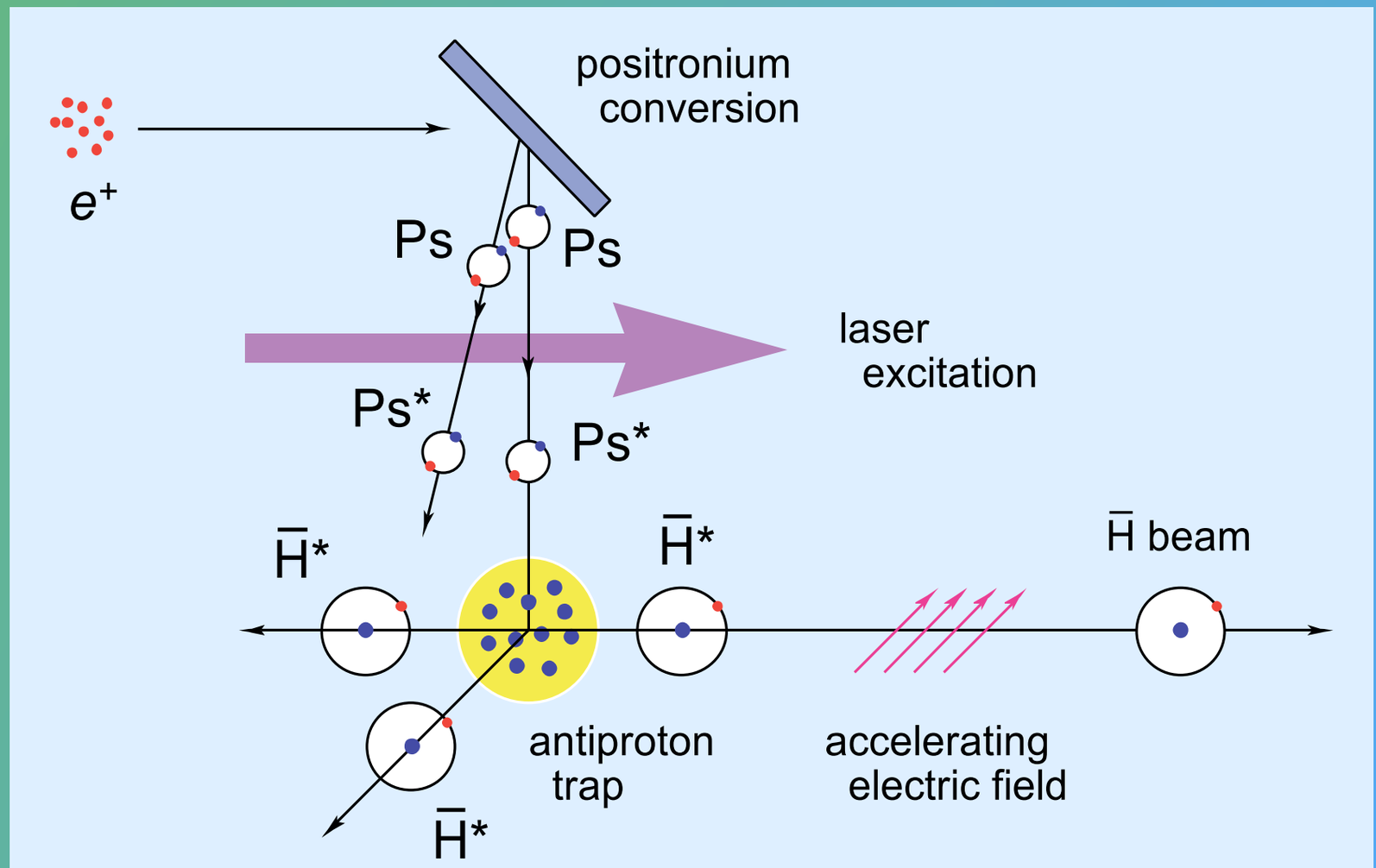

Antihydrogen will eventually be accelerated and fly toward a "moiré deflectometer"

Positronium

$$e^+ + e^- \longrightarrow Ps \longrightarrow (Ps)^*$$

Positronium [o-Ps] formation through a nanoporous silica target

Ps production efficiency $\simeq$ 27%

Mariazzi et al. Phys. Rev. Lett. 104, 243401 (2010)

e^+ implantation energy $\simeq$ 5 keV

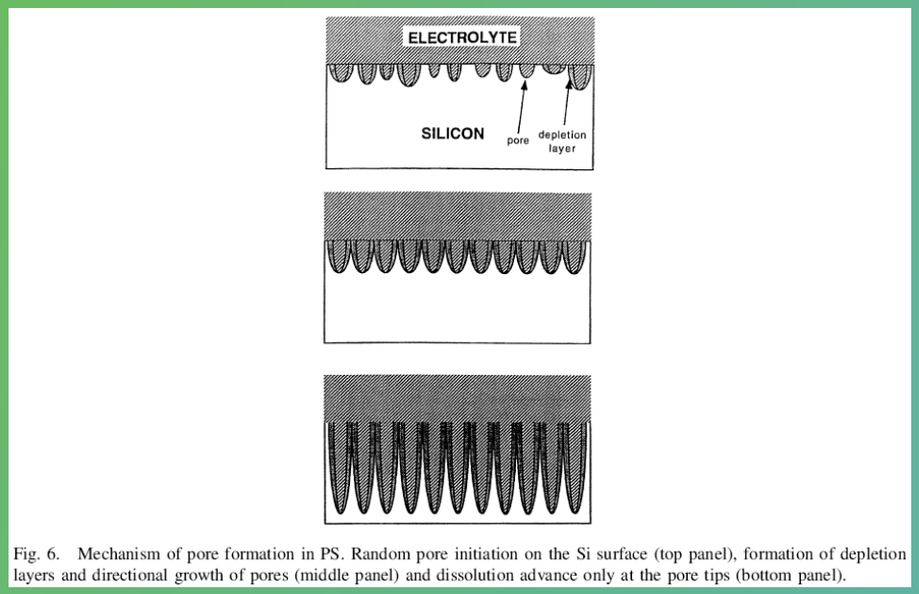

Fig. 6. Mechanism of pore formation in PS. Random pore initiation on the Si surface (top panel), formation of depletion layers and directional growth of pores (middle panel) and dissolution advance only at the pore tips (bottom panel).

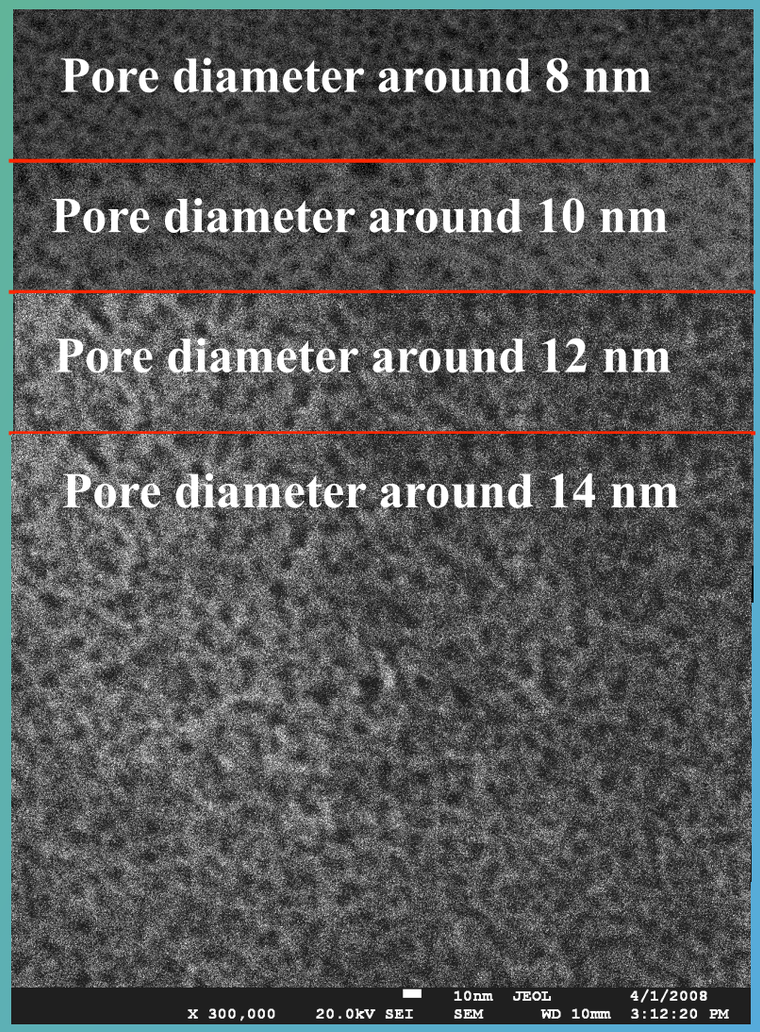

Positronium

$$e^+ + e^- \longrightarrow Ps \longrightarrow (Ps)^*$$

2 steps Positronium laser excitation

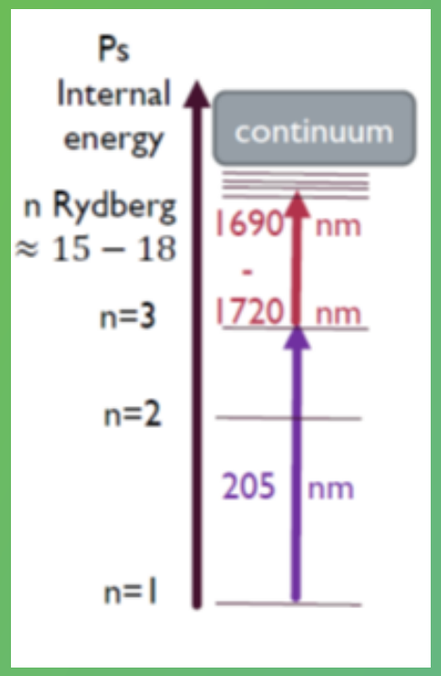

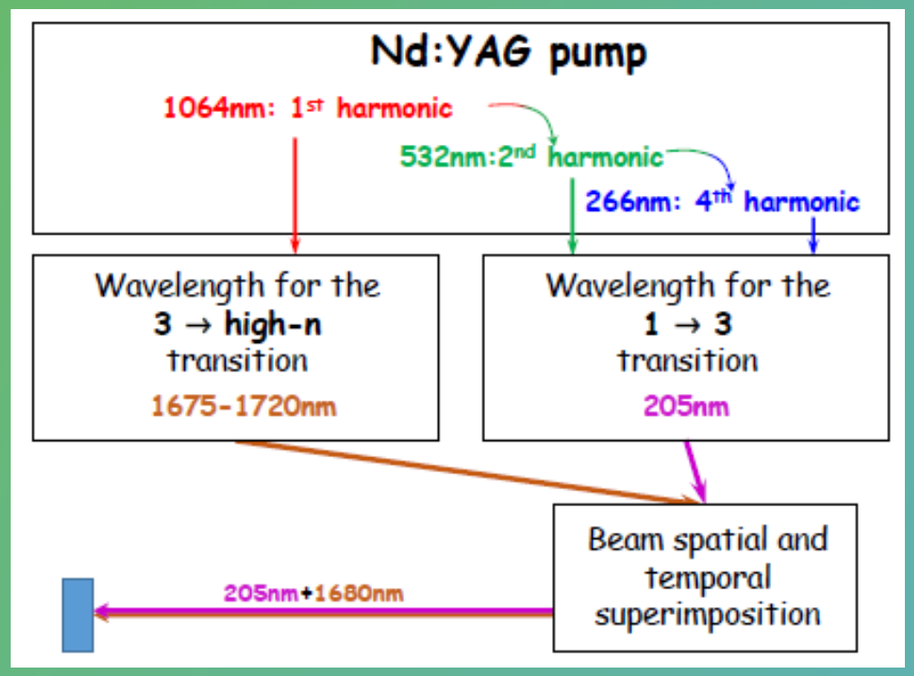

UV 205.047 nm	IR 1680-1715 nm
1.5 ns	5 ns (2 ns delay with respect to UV)
3mm FWHM	3.5 mm FWHM
90 μJ	1 mJ

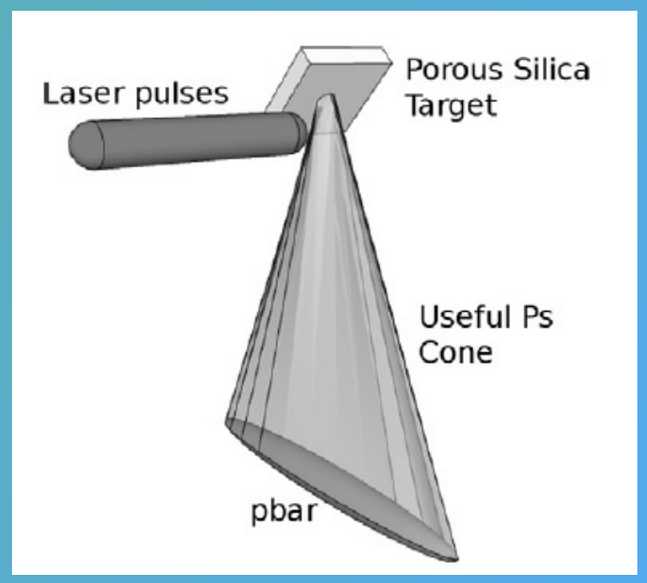

Already demonstrated by us in the e^+ test setup

"Laser excitation of the n=3 level of positronium for antihydrogen production"
Phys. Rev. A 94 (2016) 012507 AEgIS Coll.

Positronium and Rydberg Positronium formation diagnostic

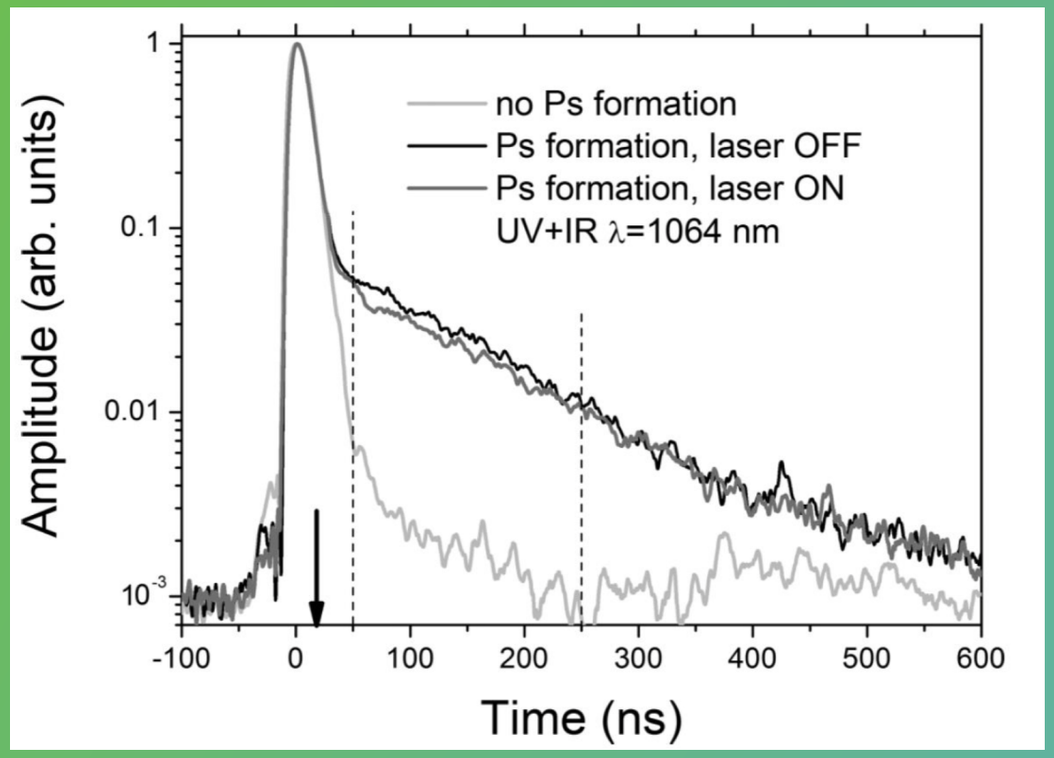

Fast detector: PbF_2 +PhotoMultiPlier
Analog output of the PMT signal digitized
(Single Shot Positron Lifetime Spectroscopy: SSPALS)
[D. B. Cassidy et al. NIMB 508 (2007) 1338]
Average of 10 measurements.

Prompt peak + tail due to Ps decay with 142 ns mean lifetime

UNFORTUNATELY THE GEOMETRY OF THE PBAR TRAP REGION IS QUITE COMPLEX

Positronium and Rydberg Positronium formation dignostics

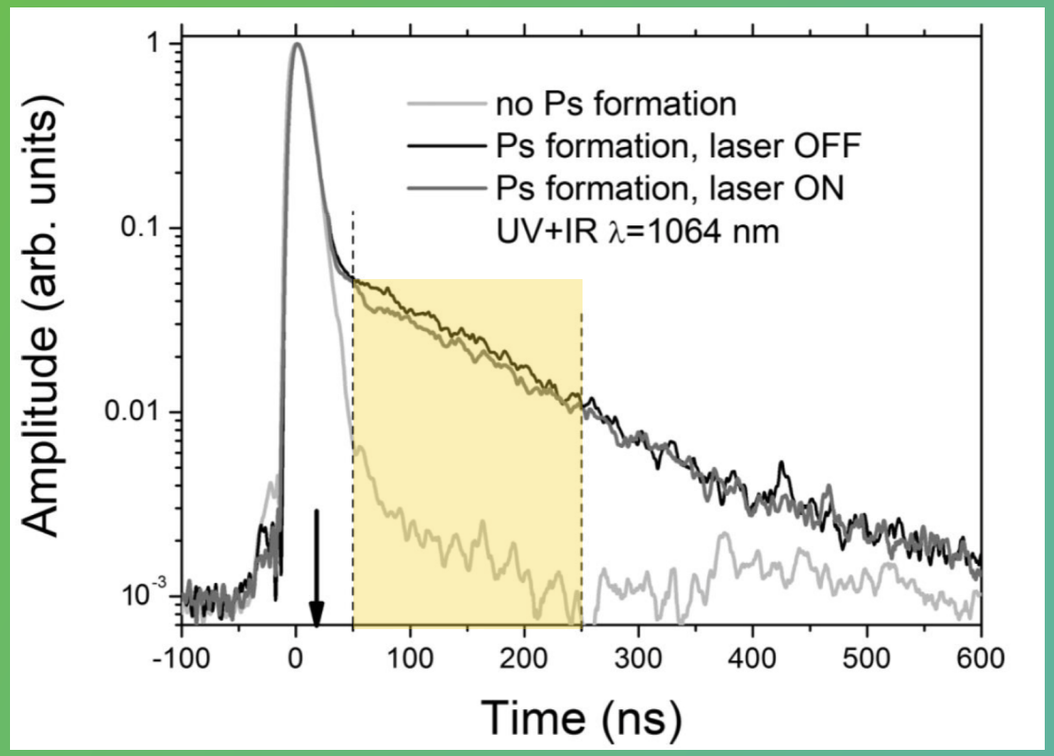

Fast detector: PbF_2 +PhotoMultiPlier
Analog output of the PMT signal digitized
(Single Shot Positron Lifetime Spectroscopy: SSPALS)
[D. B. Cassidy et al. NIMB 508 (2007) 1338]
Average of 10 measurements.

Prompt peak + tail due to Ps decay with 142 ns mean lifetime

-S(%) = (Area laser OFF-Area laser ON)/Area laser OFF

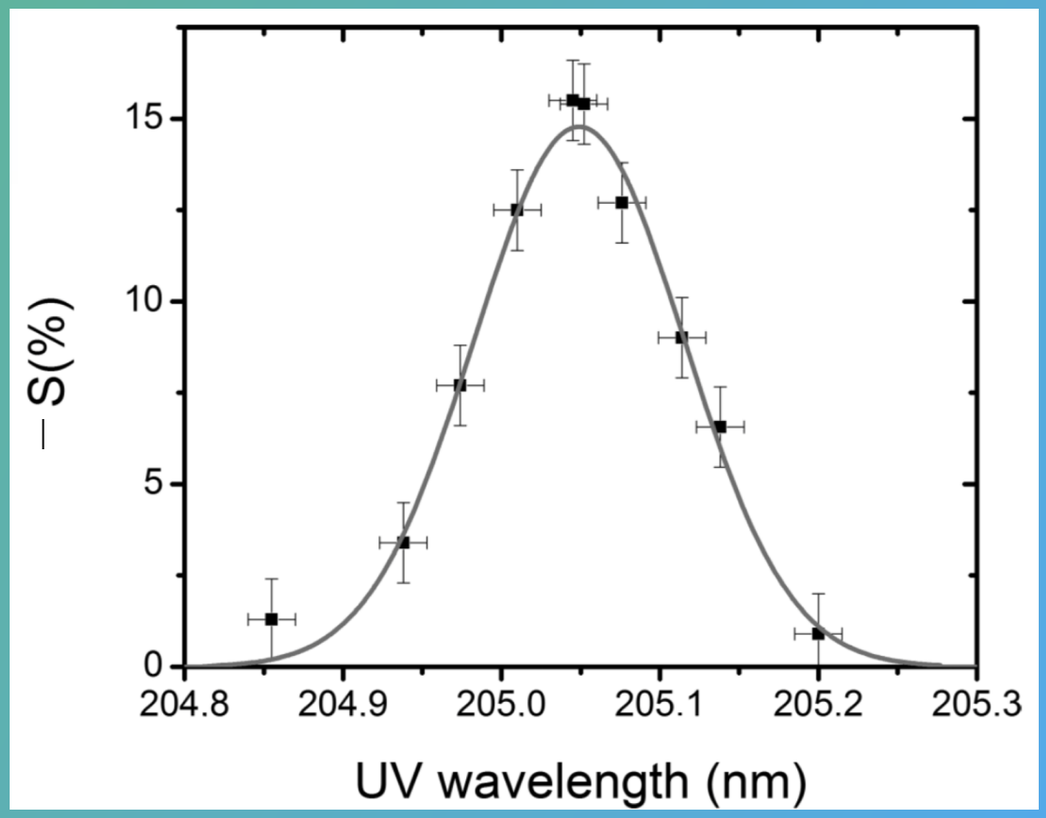

Rydberg Ps has a longer lifetime than ground state Ps
If excited, Ps atoms can reach obstacles at large distance
Practically, more annihilations are seen at later time

UNFORTUNATELY THE GEOMETRY OF THE PBAR TRAP REGION IS QUITE COMPLEX

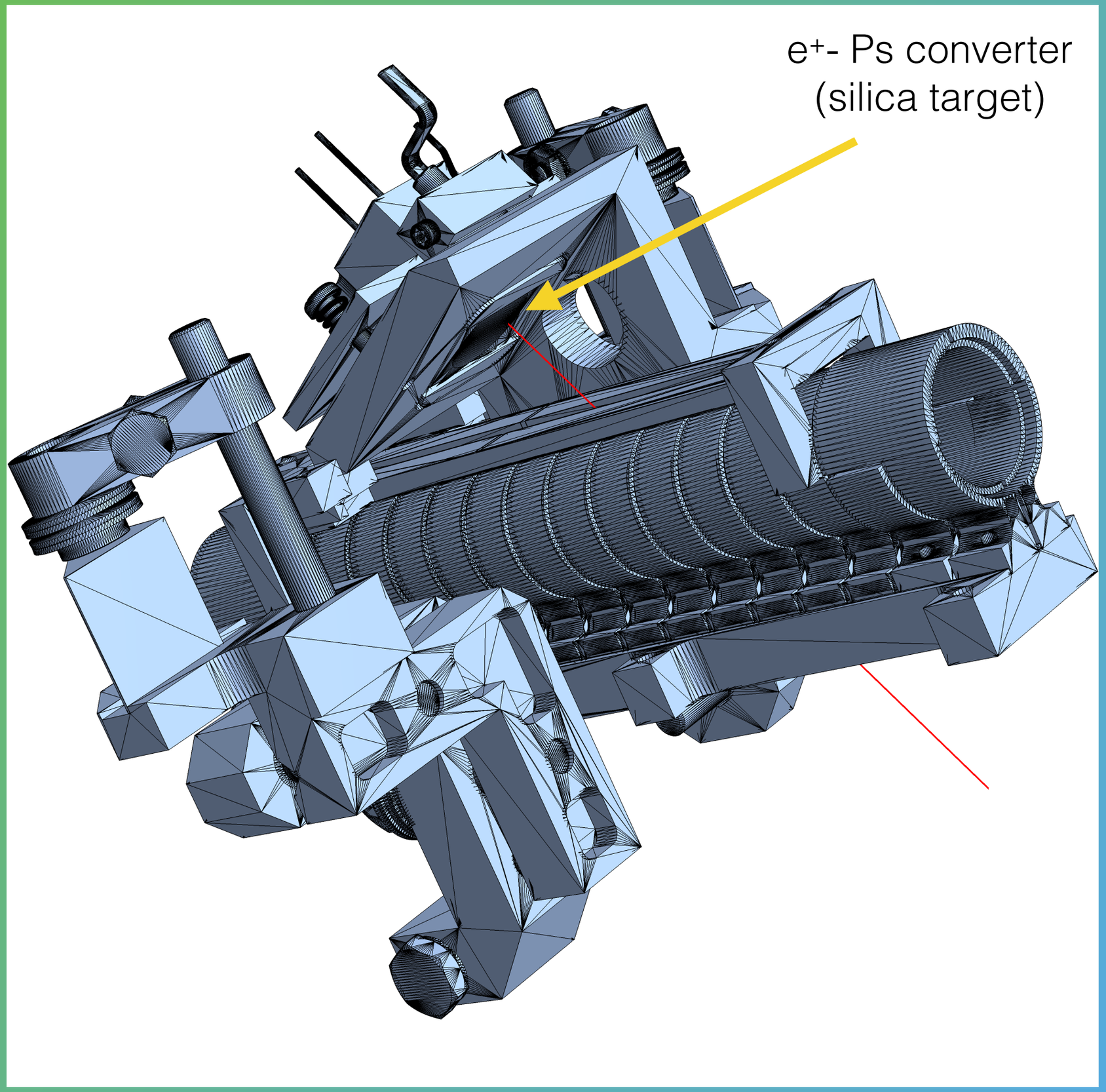
e+- Ps converter
(silica target)

AND ACTUALLY, THE FULL GEOMETRY IS EVEN MORE INTRICATE

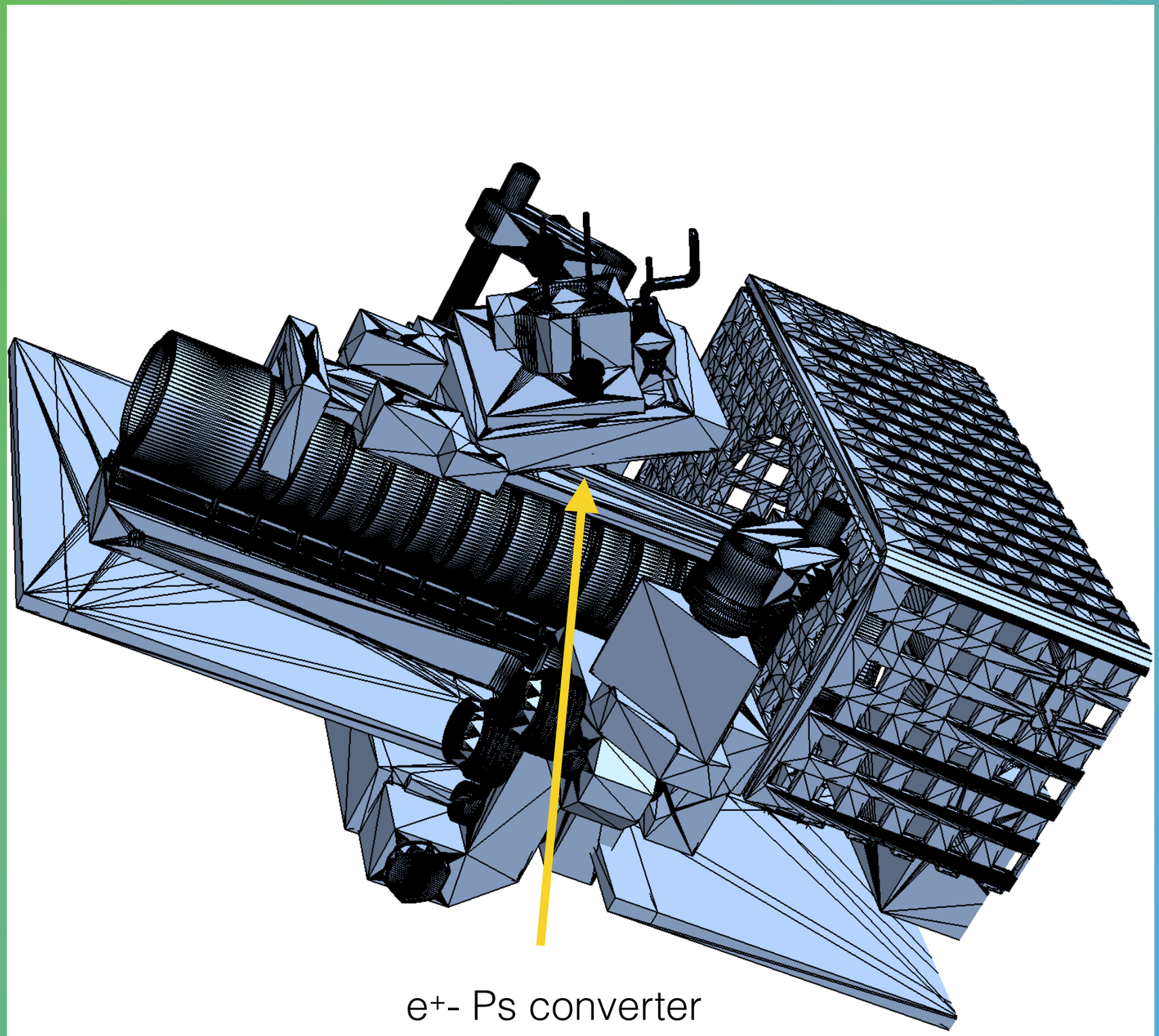

e^+- Ps converter
(silica target)

SIMULATION APPROACH:
split the problem in 2 parts

(and treat the most of the precesses analytically)

Spatial simulation (tracking)

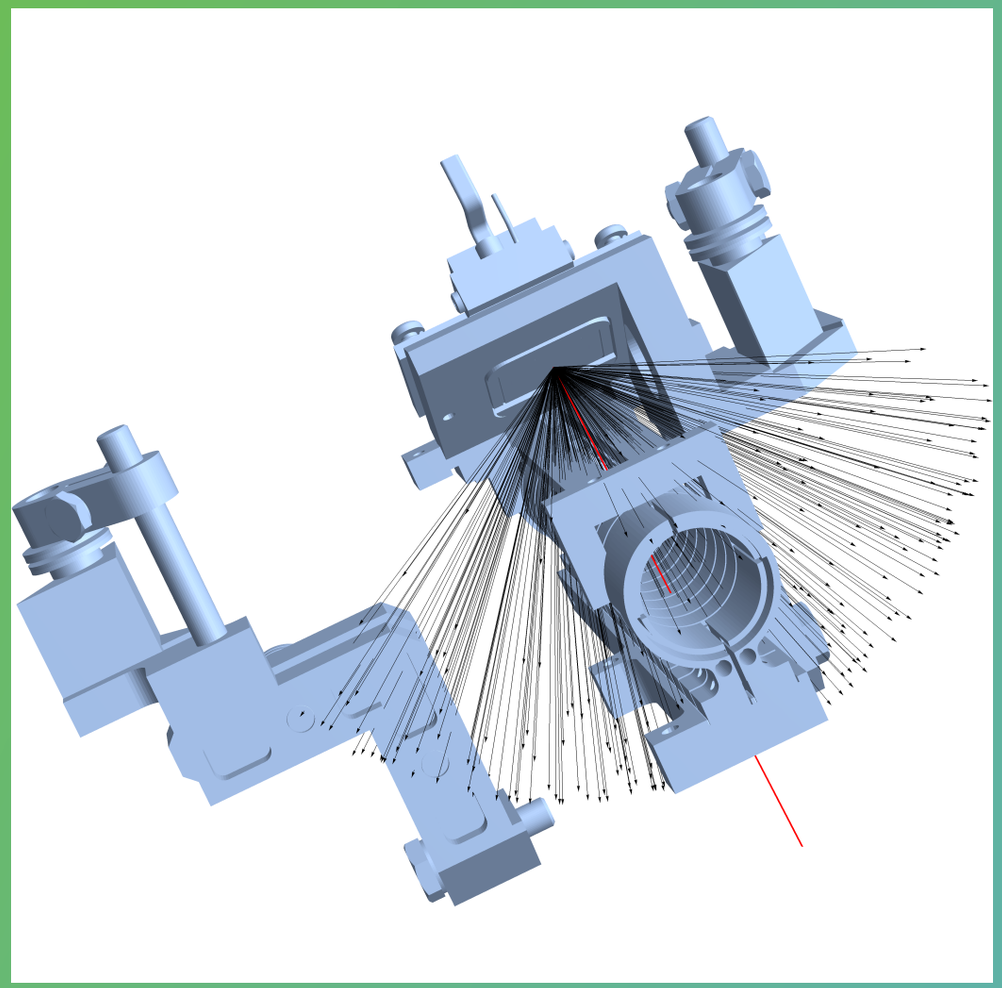

Temporal simulation: oPs lifetime

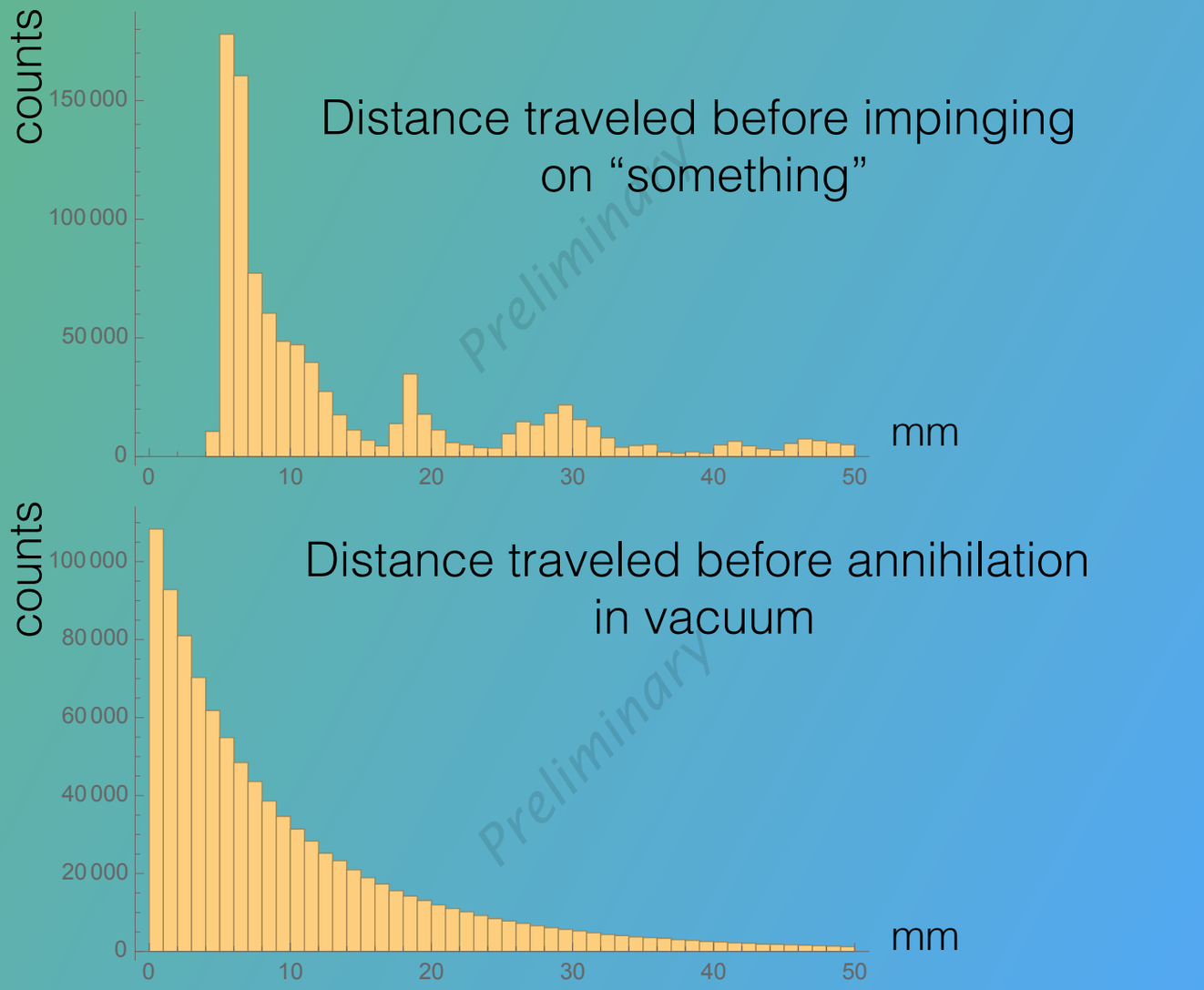

SIMULATION APPROACH:
split the problem in 2 parts

(and treat the most of the precesses analytically)

Spatial simulation (tracking)

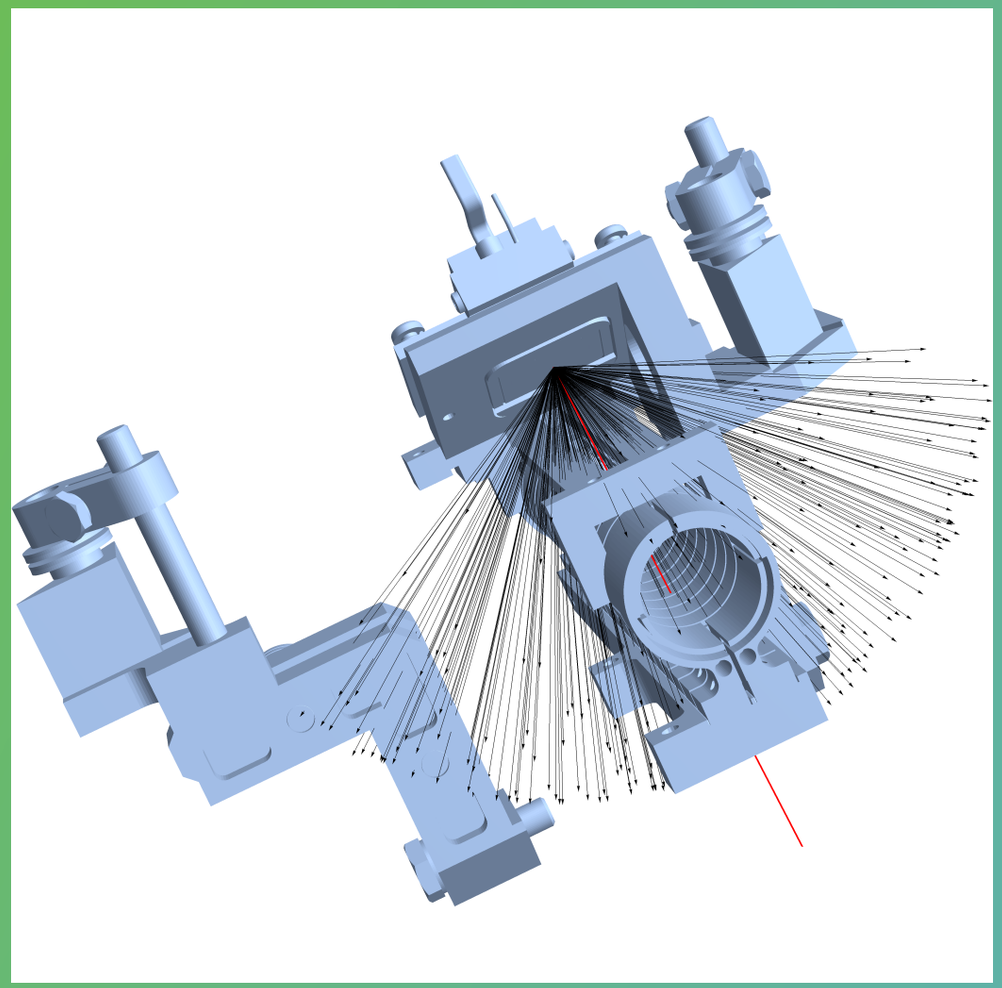

Temporal simulation: oPs lifetime

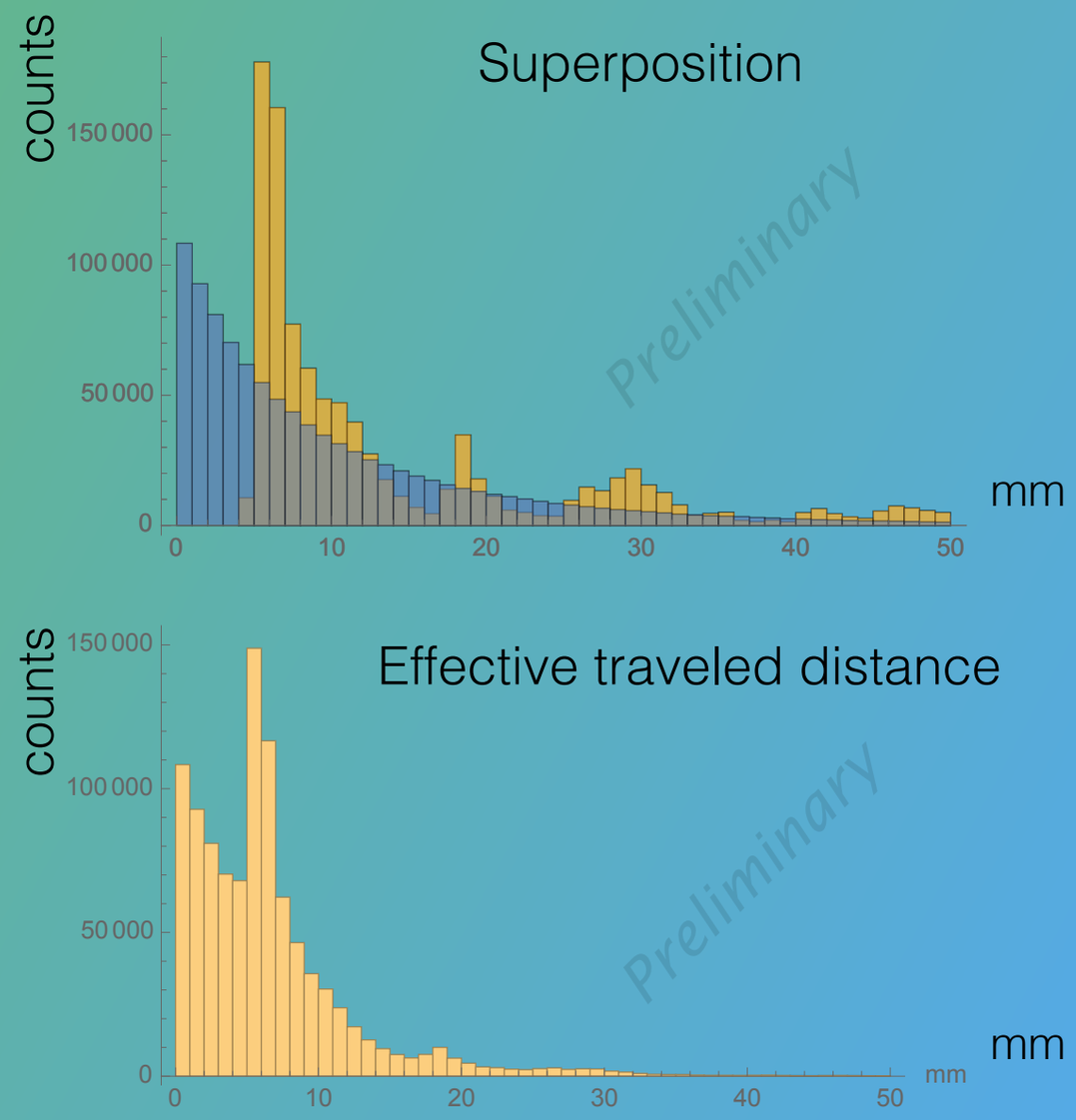

SIMULATION APPROACH:
split the problem in 2 parts

(and treat the most of the precesses analytically)

Spatial simulation (tracking)

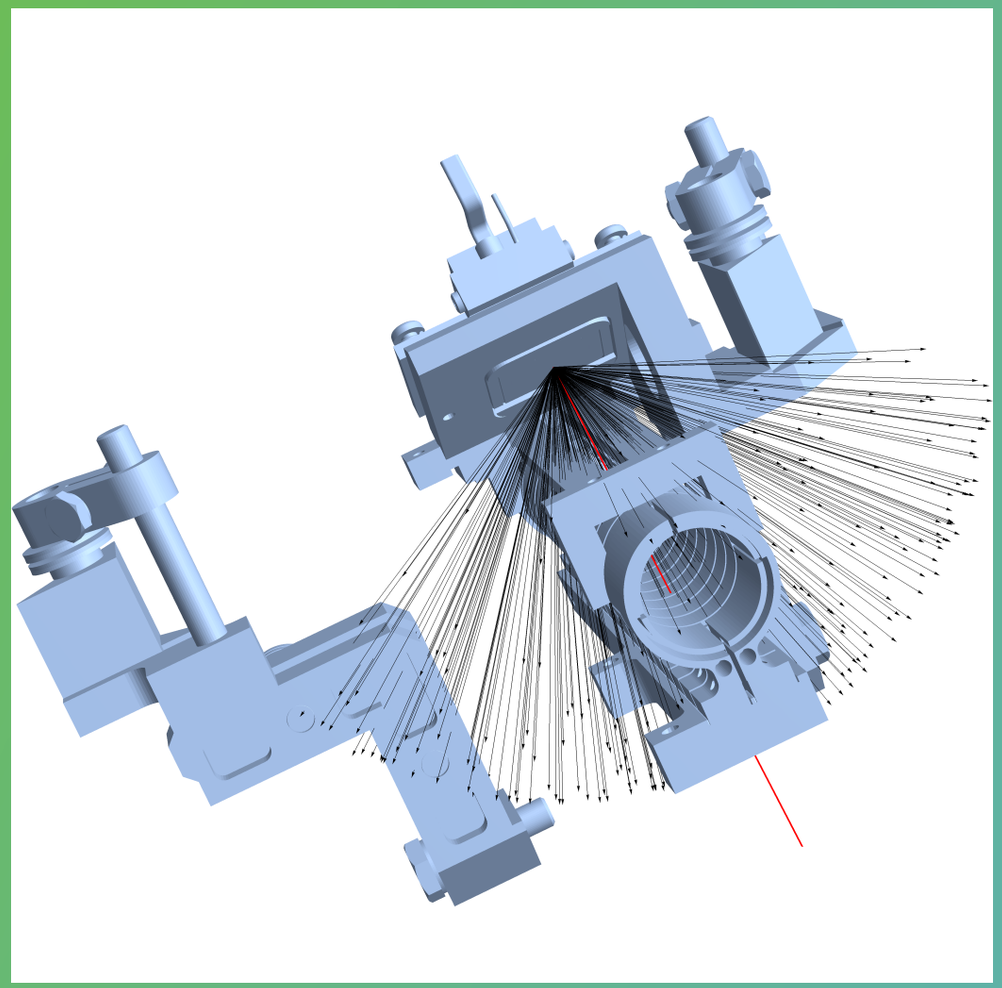

Temporal simulation: oPs lifetime

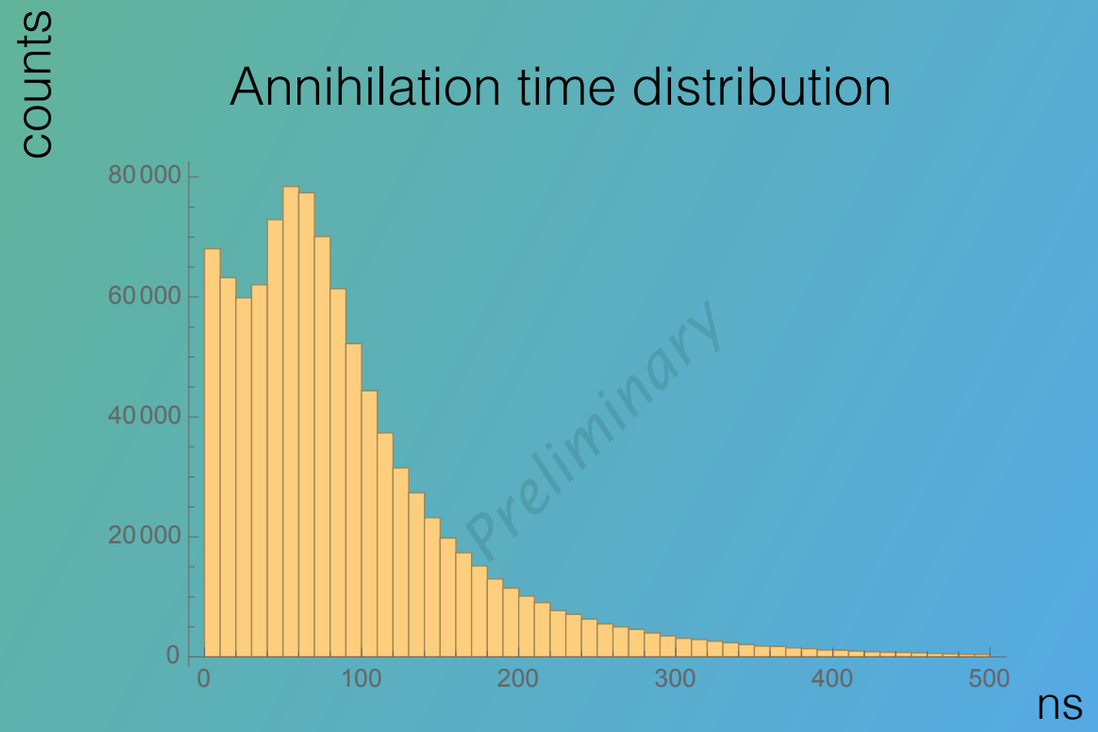

Code Scheme

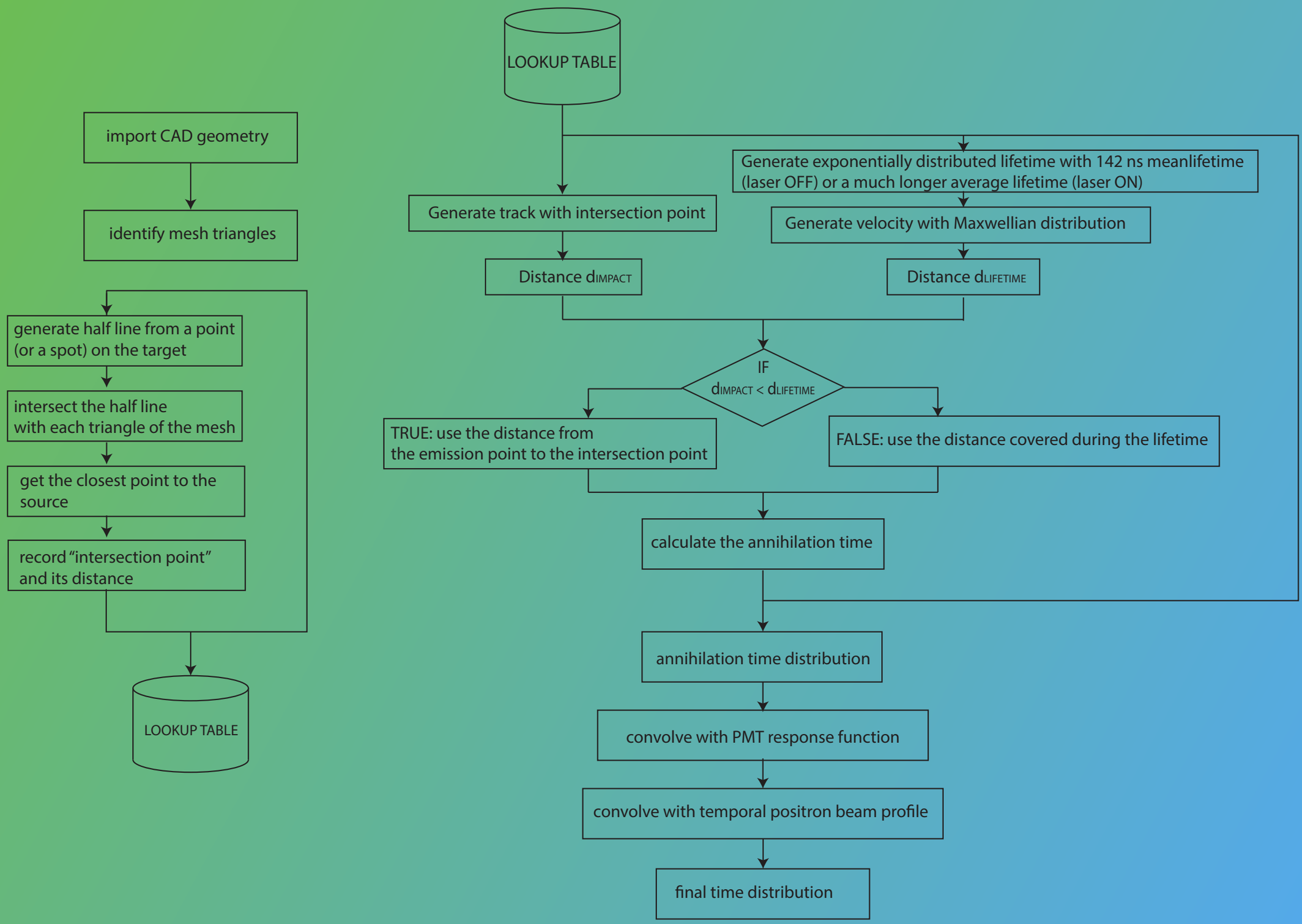

+contingent laser excitation(Rydberg Ps)

NICOLA ZURLO

AEGIS COLLABORATION

Spatial simulation

We started from the CAD drawing and noticed that
the mesh was formed by a large number of polygons, namely triangles
In this example of CAD Drawing, we have 230502 triangles

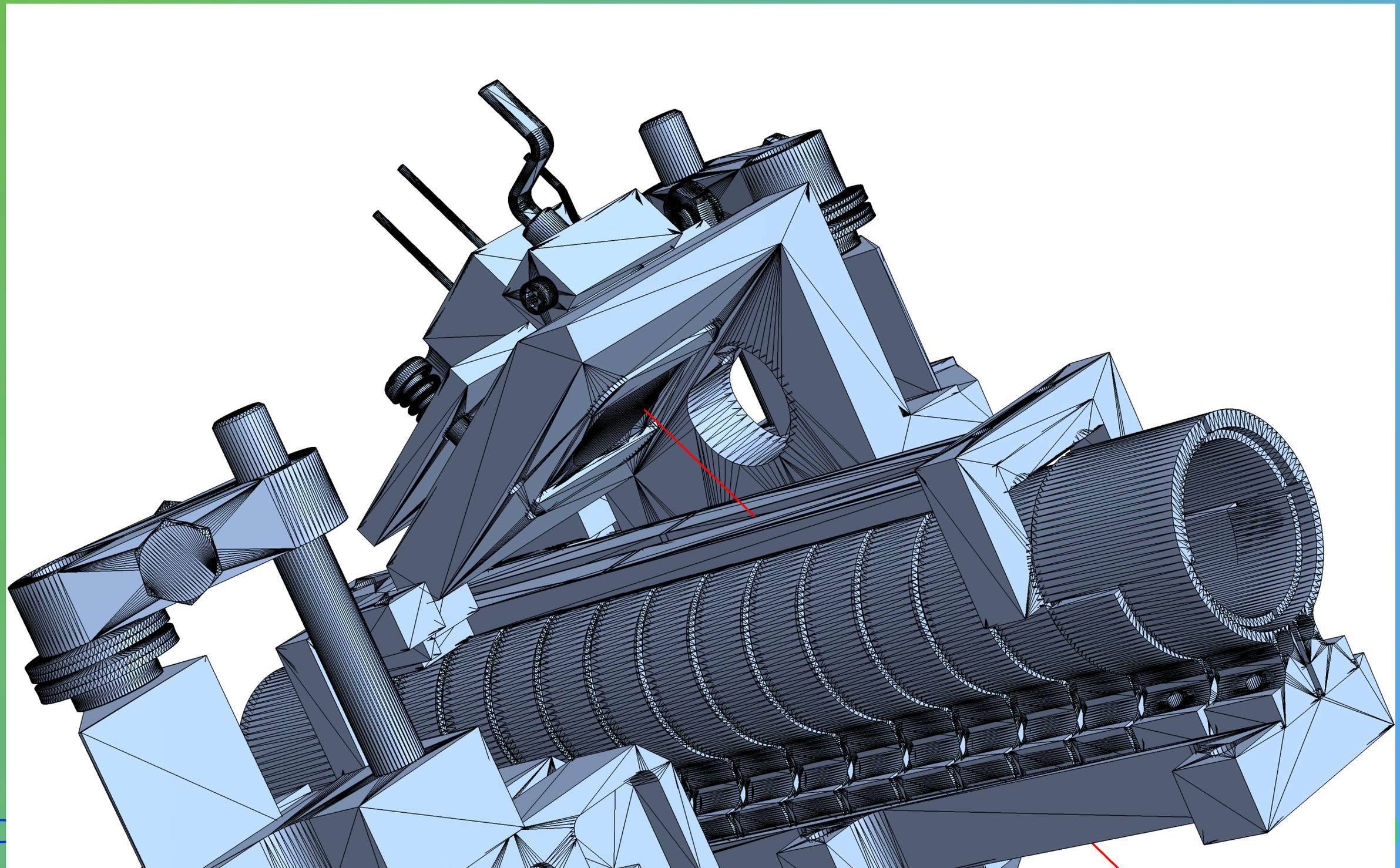

Now: the intersection of a straight line with a triangle (i.e. a plane) can be resolved analytically

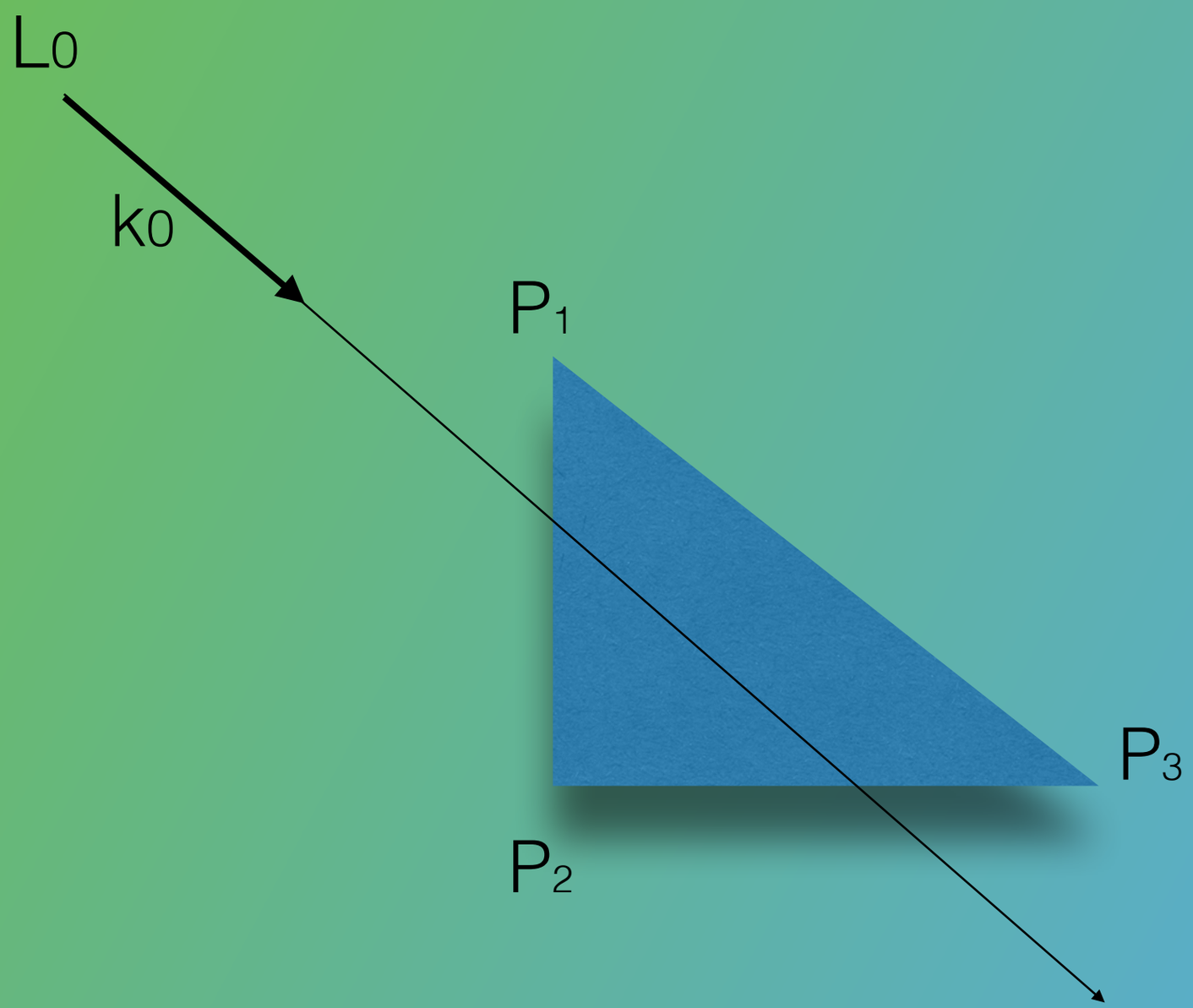

Now: the intersection of a straight line with a triangle (i.e. a plane) can be resolved analytically

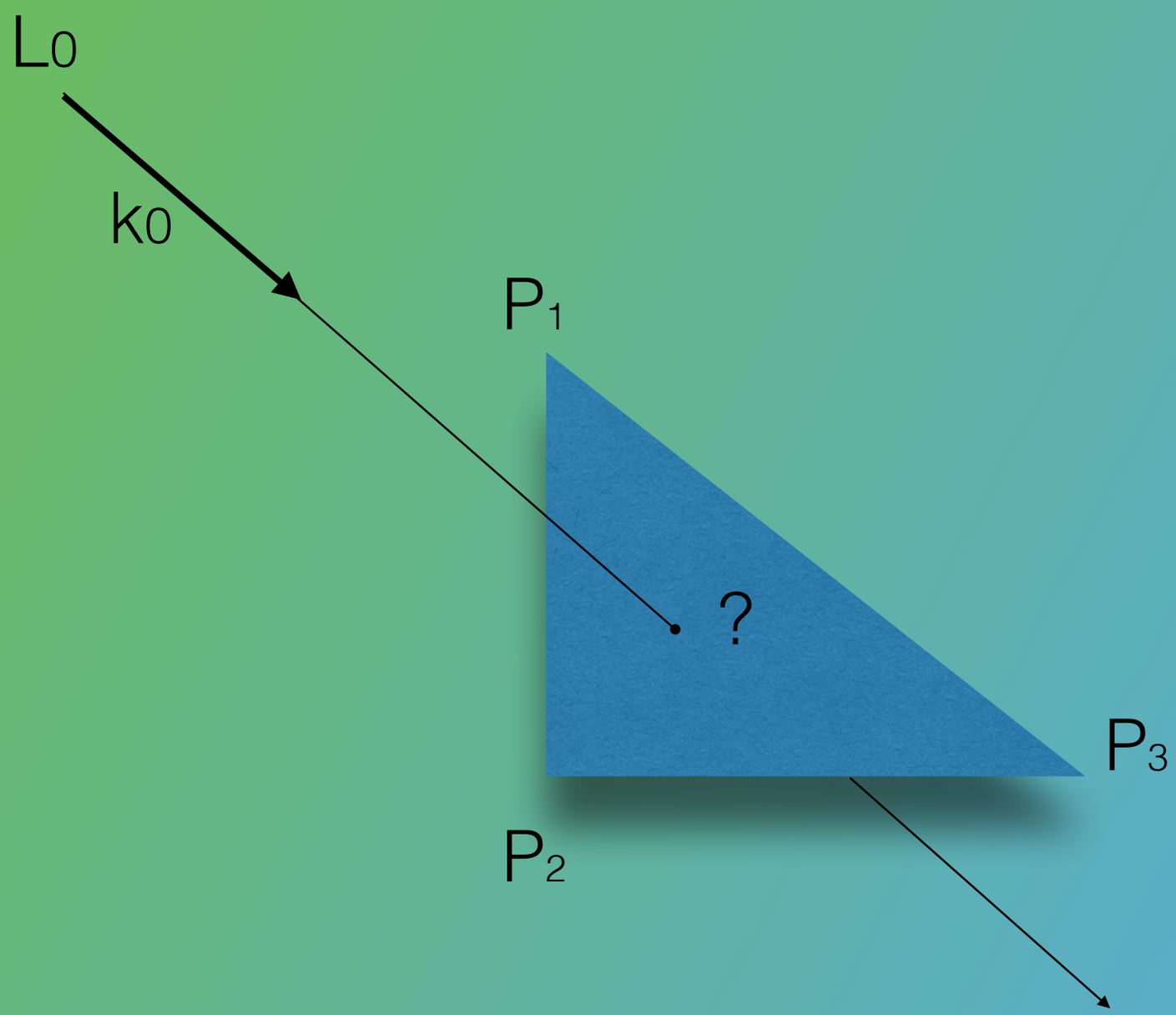

Defined: $P_1 = (P_{1x}, P_{1y}, P_{1z})$ $P_2 = (P_{2x}, P_{2y}, P_{2z})$ $P_3 = (P_{3x}, P_{3y}, P_{3z})$ and: $L_0 = (L_{0x}, L_{0y}, L_{0z})$ $\vec{k} = (k_x, k_y, k_z)$

If you introduce the auxiliary variables:

$$
\begin{aligned}
A_x &= P_{1x} - L_{0x} \\
B_x &= -P_{1x} + P_{3x} \\
C_x &= P_{2x} - P_{3x} \\
A_y &= P_{1y} - L_{0y} \\
B_y &= -P_{1y} + P_{3y} \\
C_y &= P_{2y} - P_{3y} \\
A_z &= P_{1z} - L_{0z} \\
B_z &= -P_{1z} + P_{3z} \\
C_z &= P_{2z} - P_{3z}
\end{aligned}
$$

and then define:

$$t^* = \frac{A_z B_y C_x - A_y B_z C_x - A_z B_x C_y + A_x B_z C_y + A_y B_x C_z - A_x B_y C_z}{B_z C_y k_x - B_y C_z k_x - B_z C_x k_y + B_x C_z k_y + B_y C_x k_z - B_x C_y k_z}$$

the coordinates of the point S of intersection of the straightline with the plane passing through P_1,P_2,P_3 are

$$S_x = k_x t^* + L_{0x}$$
$$S_y = k_y t^* + L_{0y}$$
$$S_z = k_z t^* + L_{0z}$$

Generally speaking the point S belongs to the plane but not to the triangle.

If you introduce 2 more auxiliary variables:

$$\alpha = \frac{-A_z B_y k_x + A_y B_z k_x + A_z B_x k_y - A_x B_z k_y - A_y B_x k_z + A_x B_y k_z}{A_z C_y k_x - A_y C_z k_x - A_z C_x k_y + A_x C_z k_y + A_y C_x k_z - A_x C_y k_z}$$
$$\beta = \frac{-A_z C_y k_x + A_y C_z k_x + A_z C_x k_y - A_x C_z k_y - A_y C_x k_z + A_x C_y k_z}{B_z C_y k_x - B_y C_z k_x - B_z C_x k_y + B_x C_z k_y + B_y C_x k_z - B_x C_y k_z}$$

inside the triangle means:

$0 \leqq \alpha \leqq 1$ $\qquad$ $0 \leqq \beta \leqq 1$ $\qquad$ $t > 0$

In general, non just 1 mesh triangle has intersection with the assigned straight line, but we can define the impact point as the closest intersection post to the starting point

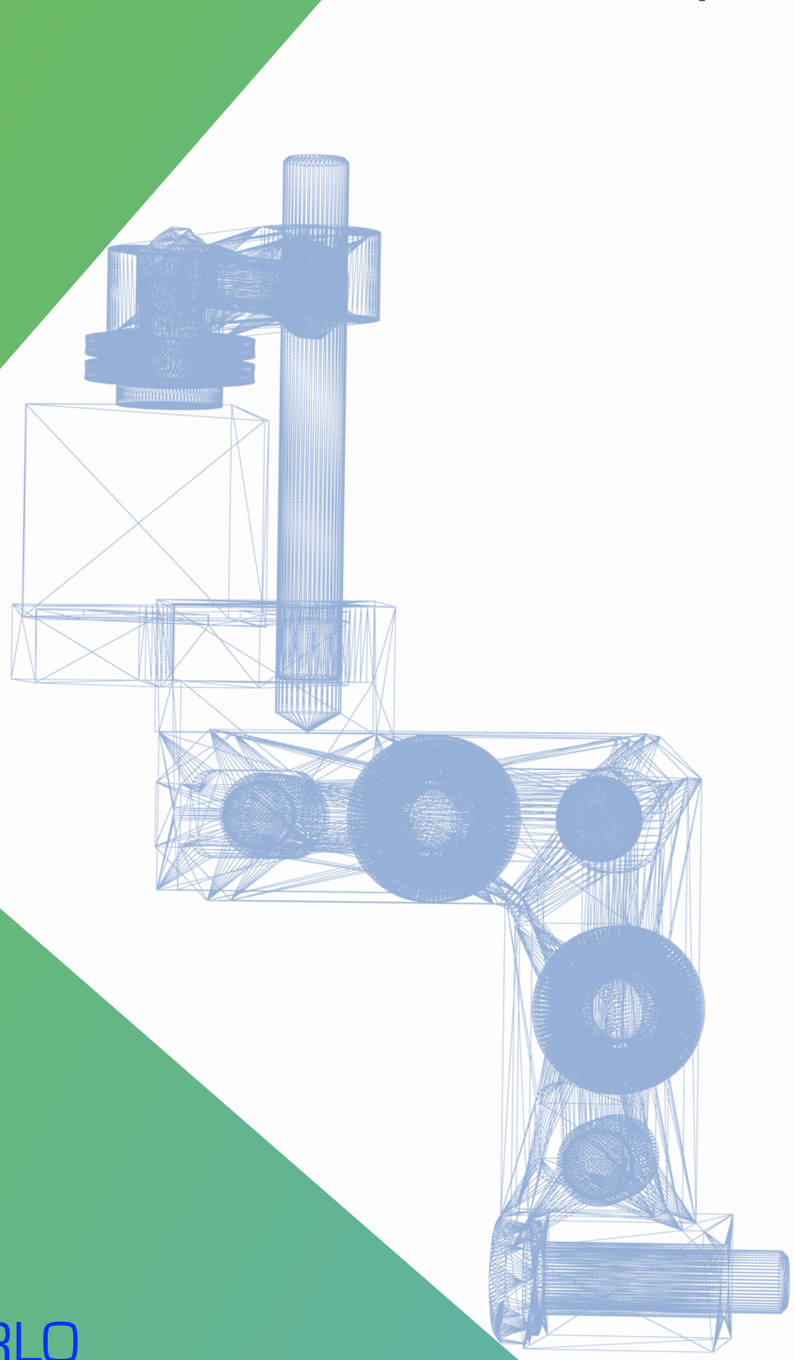

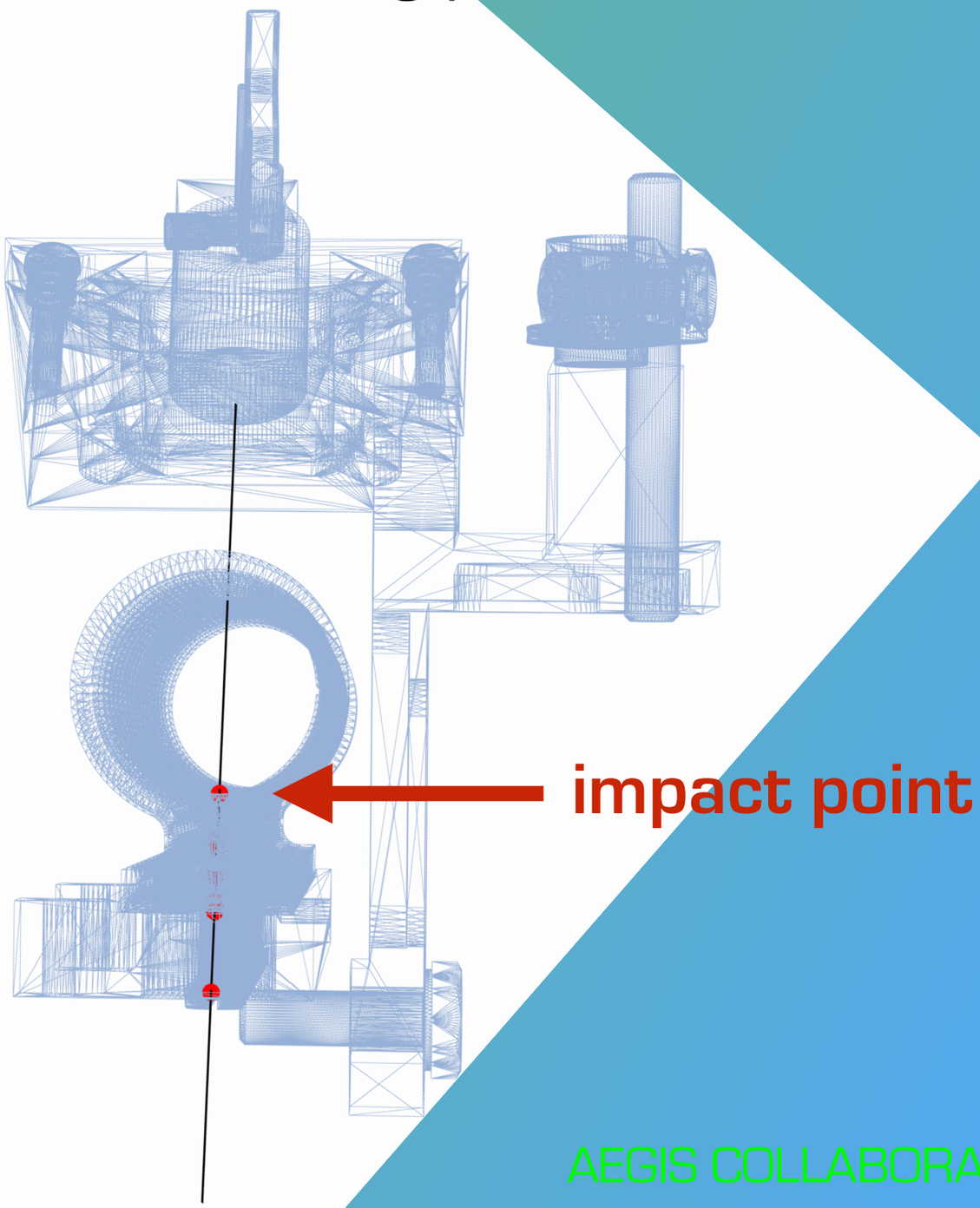

We randomly generate the straight lines from a point (or from an area, because of the e+ spatial spread) in a cone with 60° opening angle with axis perpendicular to the target plane

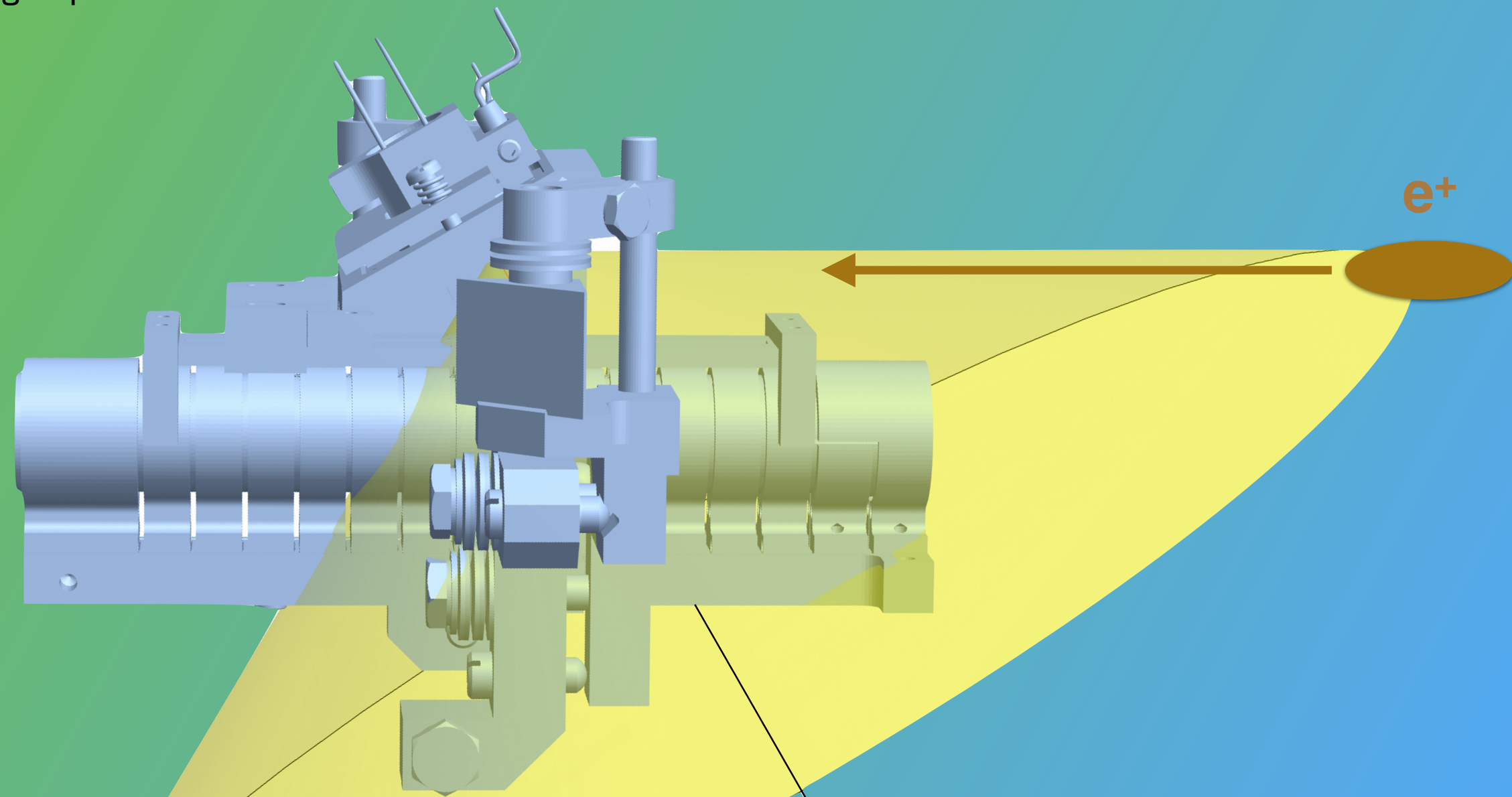

To be more precise, we introduce a spatial spread of Ps emission points in agreement with the measured positron bunch cross section
(σ_x = 0.28; σ_y = 0.13 mm)

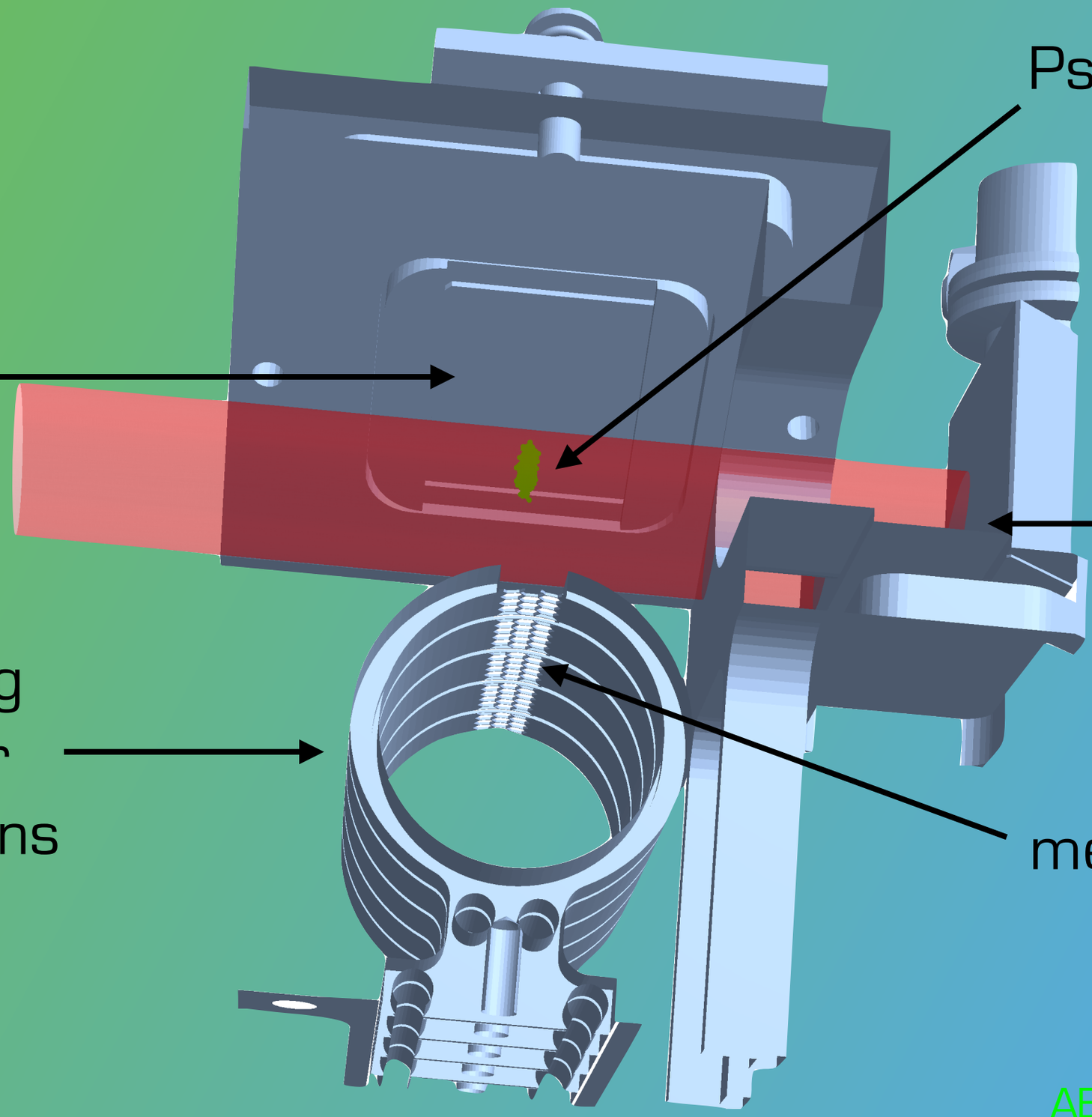

Temporal simulation

Takes into account:

- prompt annihilations at the e^+ impact on the target (≃75%)
- Ps formation (≃25% oPs with mean lifetime 142 ns)
- random lifetime → annihilation in the impact point or before depending on the lifetime
- Ps velocity distribution (thermal Maxwellian/other distributions may be implemented)
- response of the scintillator

And also:

- temporal spread of the e^+ bunch (σ_t=6 ns)
- permanence time of the Ps inside the nanopores before being released
- laser excitation of Ps to Rydberg states of much longer lifetime (Ps*)
- realistic model for the laser efficiency

Simulation of the laser efficiency

- Real laser beam position and timing (laser delay with respect to the prompt annihilation peak, set by the operator, and laser duration, around 1,5 ns)
- Detection of the Ps that are in the laser beam at the “right” time
- Excitation probability linked to the time in which the Ps “sees” the laserlight and to the R frequency
- Doppler Effect taken into account (depending on the Ps parallel velocity and on the laser bandwidth)
- Possible limit of the current analytical approach : top-hat laser beam profile

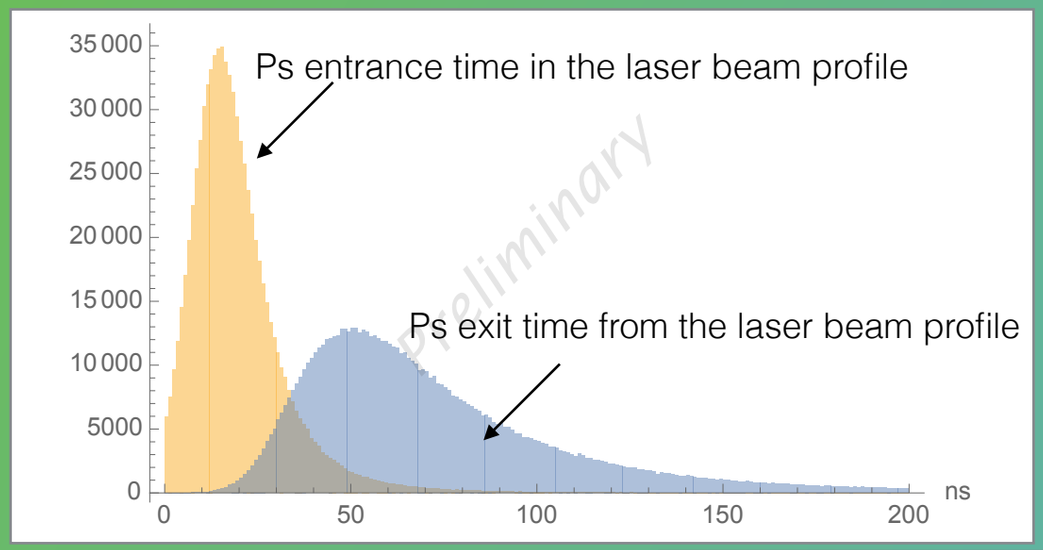

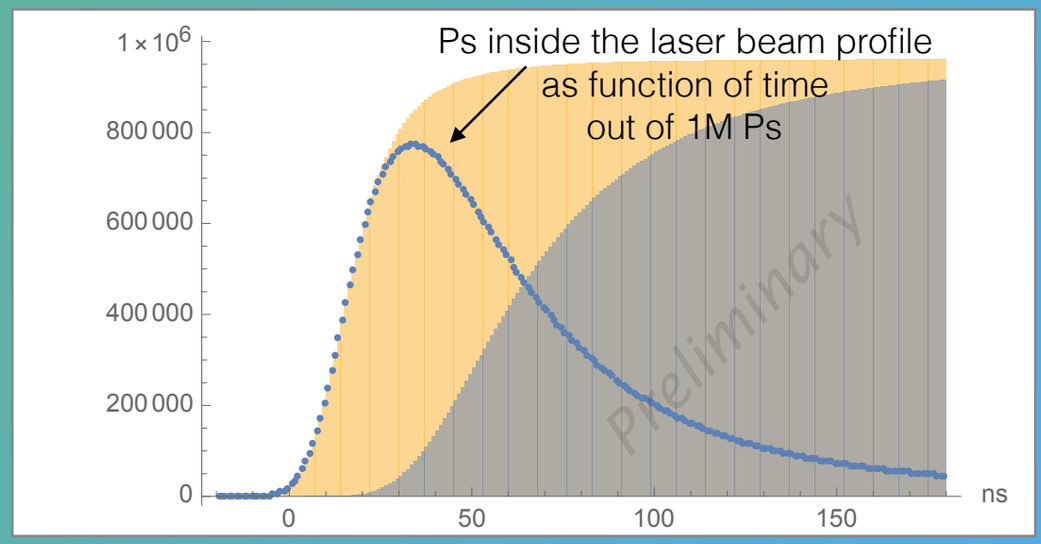

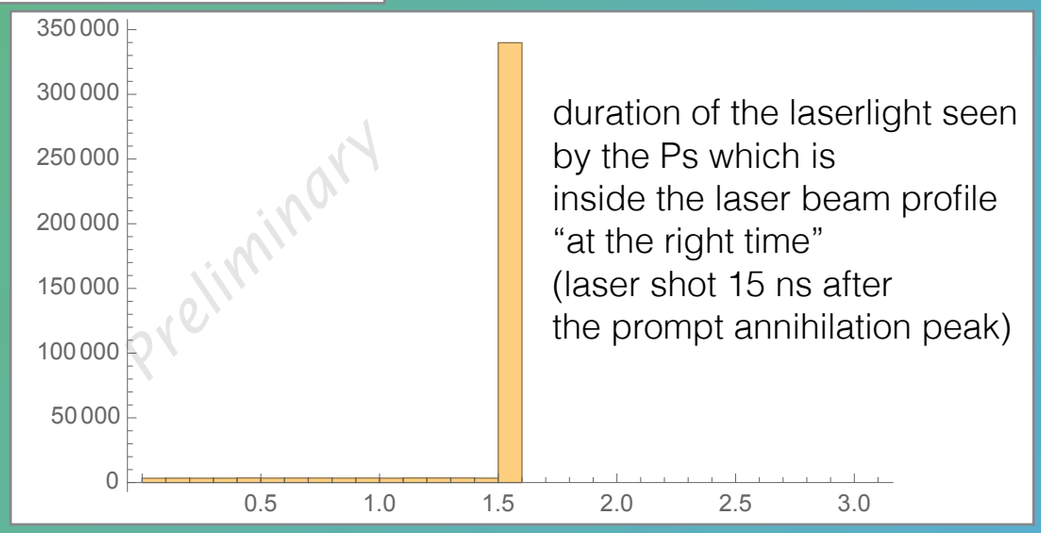

NB. In those and the next figures
Ps emission T
supposed 300 K

Laser fired 45 ns after the prompt

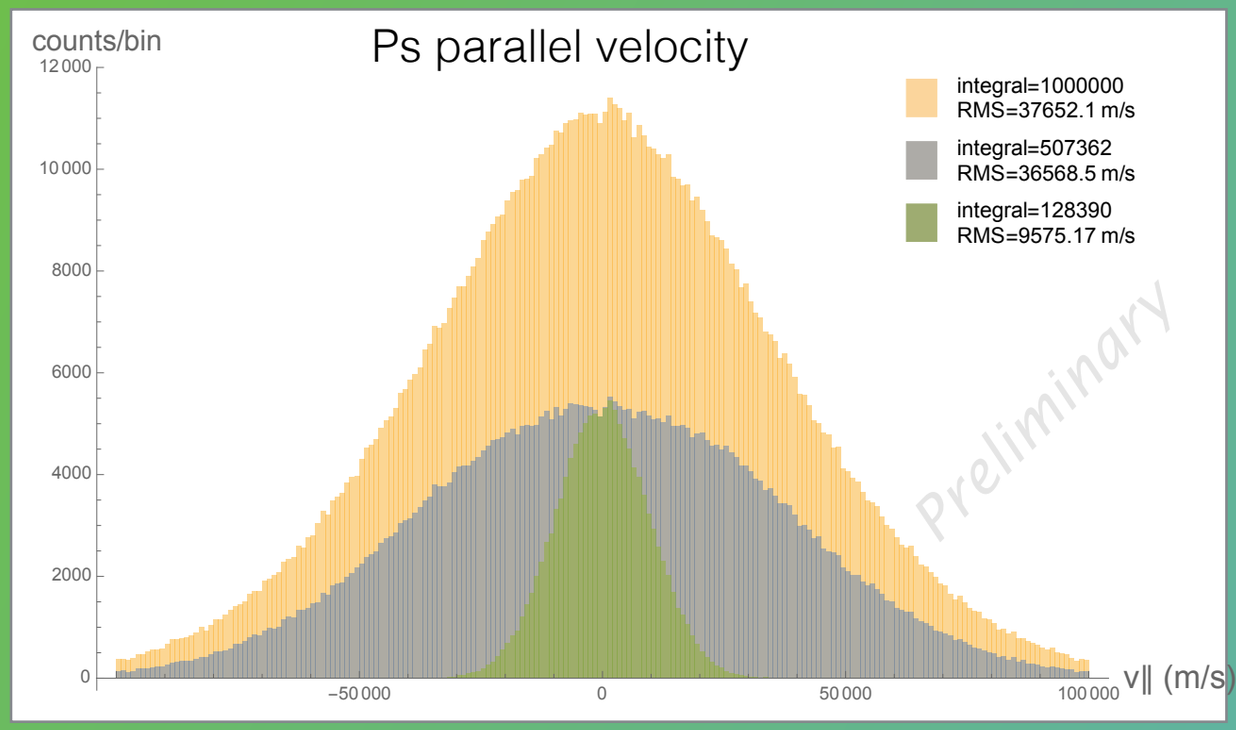

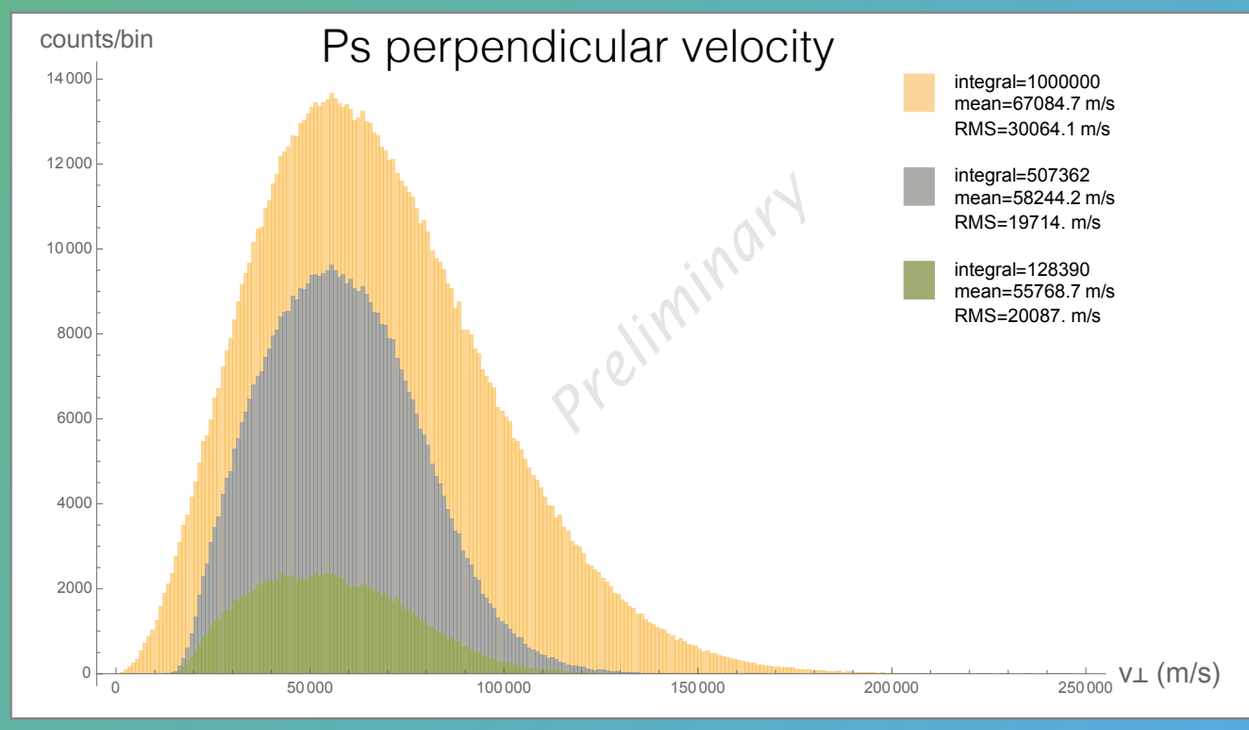

Ps velocity distribution
when emitted from the target

Ps velocity distribution
of the ones illuminated by the laser

Rydberg excited Ps*
velocity distribution

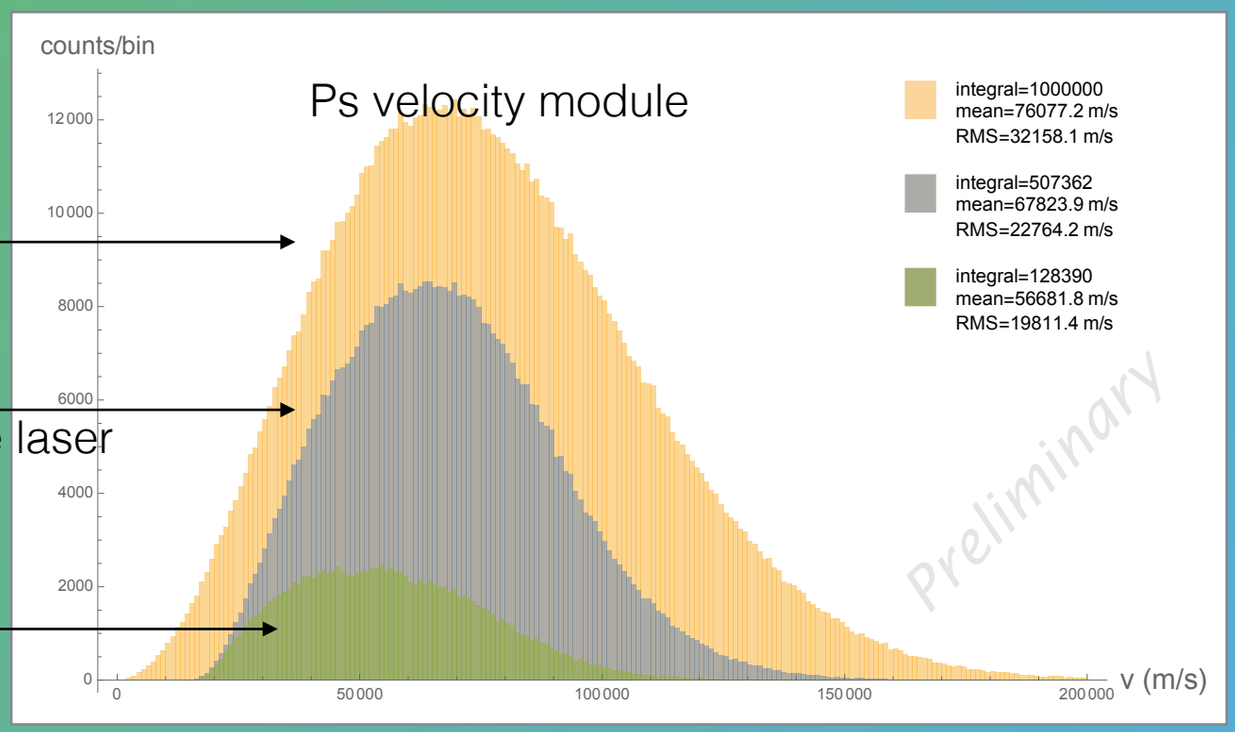

What about the SSPALS?
If we had only Ps and Ps*…

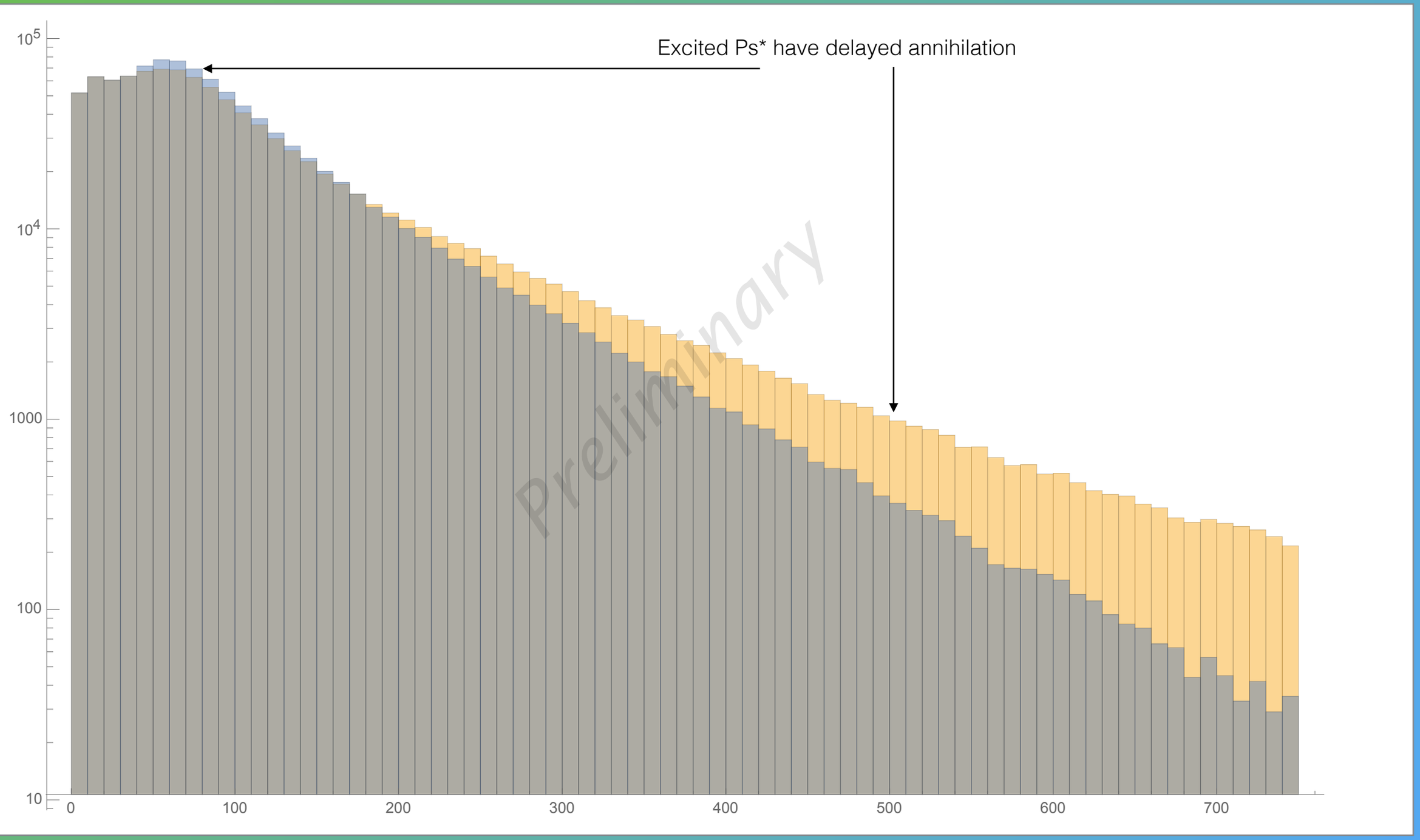

… but what we actually measure has convoluted the prompt annihilation and the scintillator function response

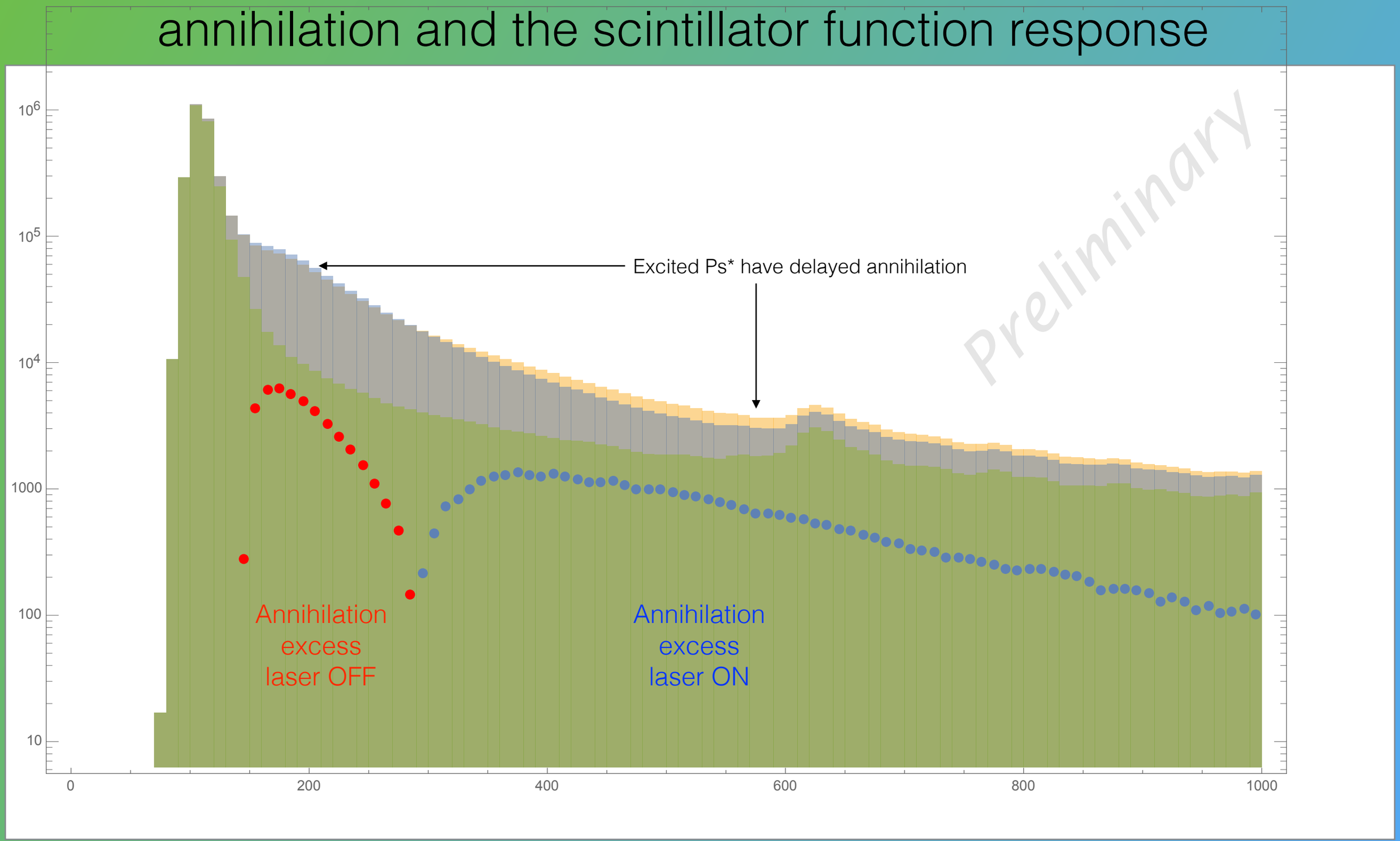

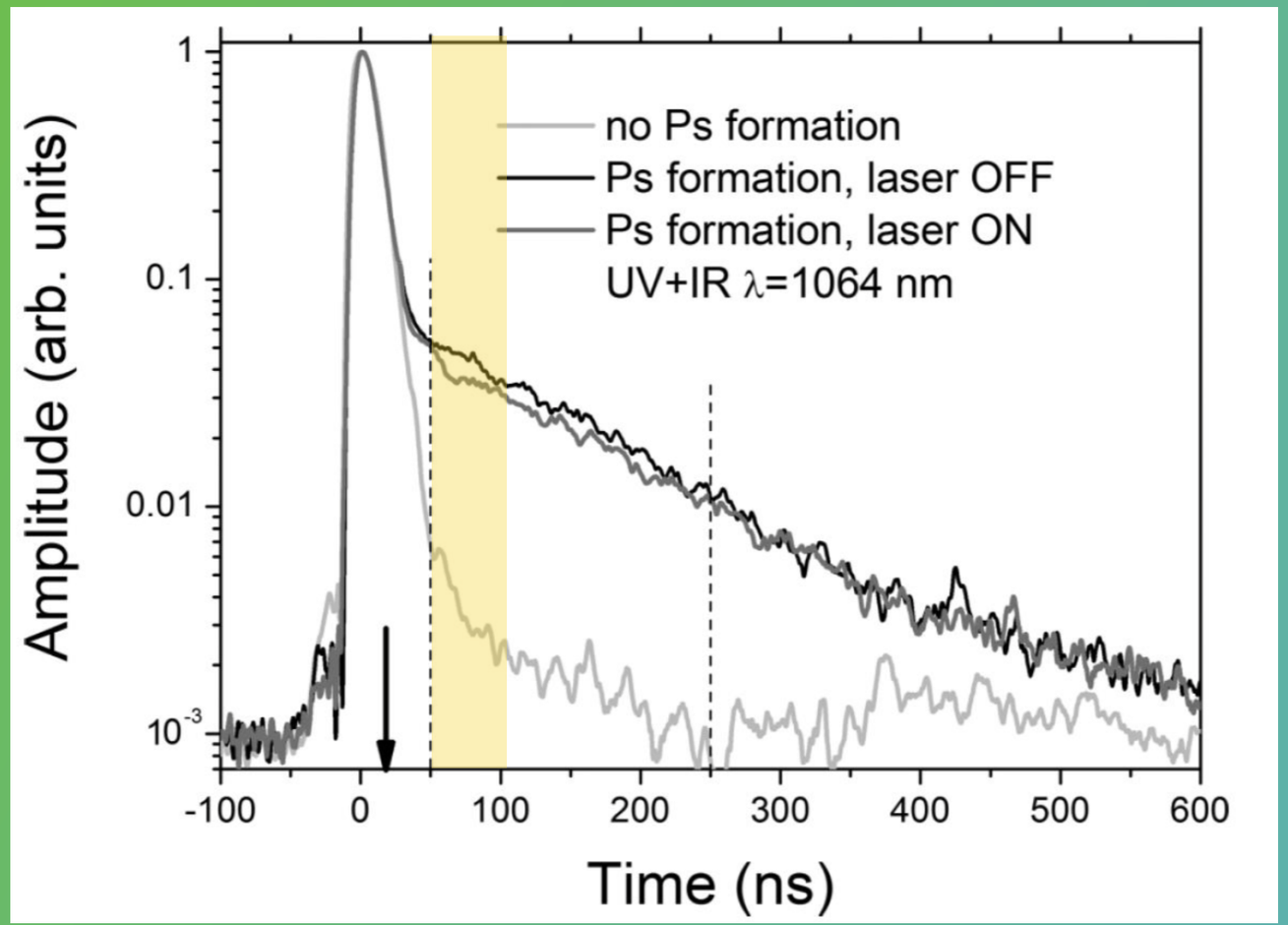
Amplitude (arb. units)
1
0.1
0.01
10^{-3}
no Ps formation
Ps formation, laser OFF
Ps formation, laser ON
UV+IR λ=1064 nm
-100
0
100
200
300
400
500
600
Time (ns)

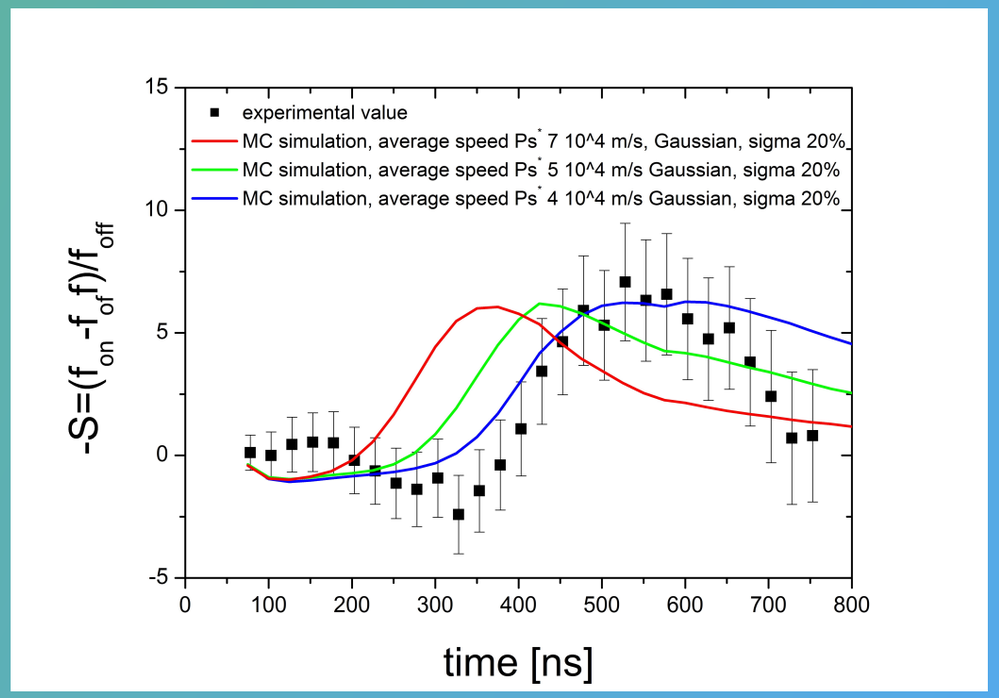
experimental value
MC simulation, average speed Ps* 7 10^4 m/s, Gaussian, sigma 20%
MC simulation, average speed Ps* 5 10^4 m/s Gaussian, sigma 20%
MC simulation, average speed Ps* 4 10^4 m/s Gaussian, sigma 20%
$-S=(f_{on}-f_{of}f)/f_{off}$
15
10
5
0
-5
0
100
200
300
400
500
600
700
800
time [ns]

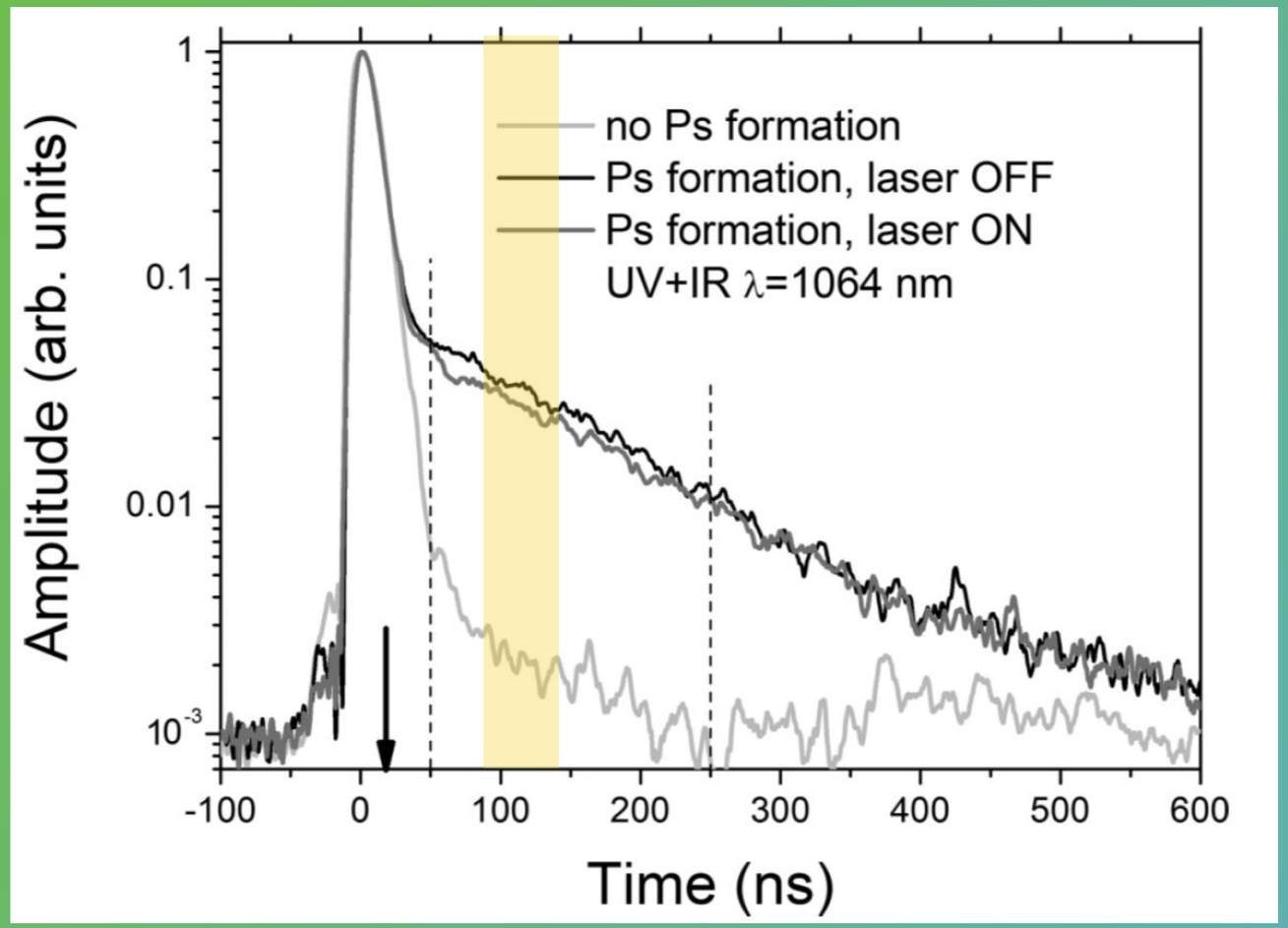
Amplitude (arb. units)
1
0.1
0.01
10^{-3}
no Ps formation
Ps formation, laser OFF
Ps formation, laser ON
UV+IR λ=1064 nm
-100
0
100
200
300
400
500
600
Time (ns)

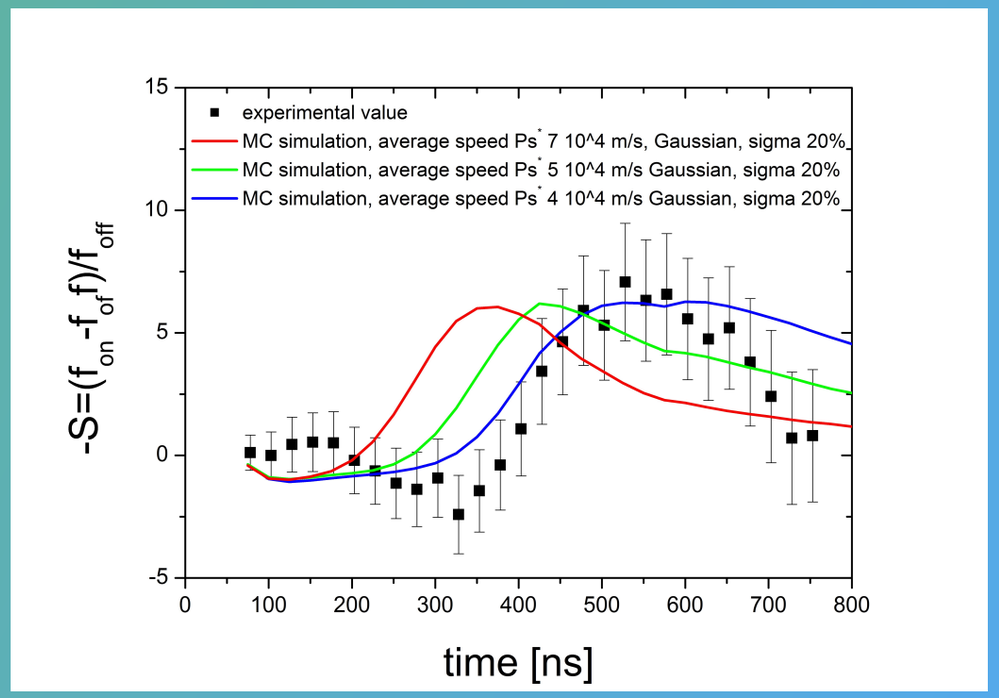
experimental value
MC simulation, average speed Ps* 7 10^4 m/s, Gaussian, sigma 20%
MC simulation, average speed Ps* 5 10^4 m/s Gaussian, sigma 20%
MC simulation, average speed Ps* 4 10^4 m/s Gaussian, sigma 20%
$-S=(f_{on}-f_{of}f)/f_{off}$
15
10
5
0
-5
0
100
200
300
400
500
600
700
800
time [ns]

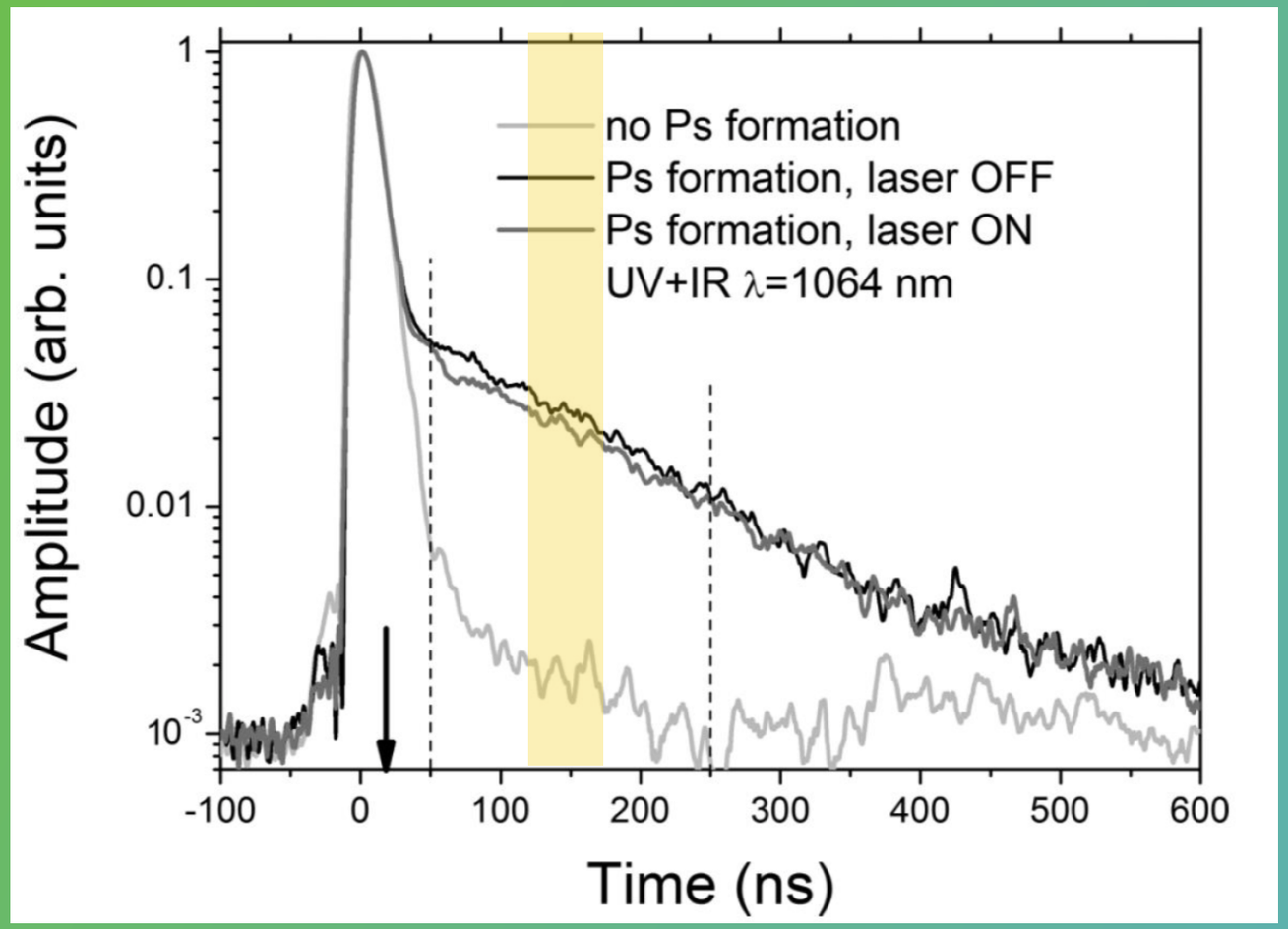
Amplitude (arb. units)
1
0.1
0.01
10^{-3}
no Ps formation
Ps formation, laser OFF
Ps formation, laser ON
UV+IR λ=1064 nm
-100
0
100
200
300
400
500
600
Time (ns)

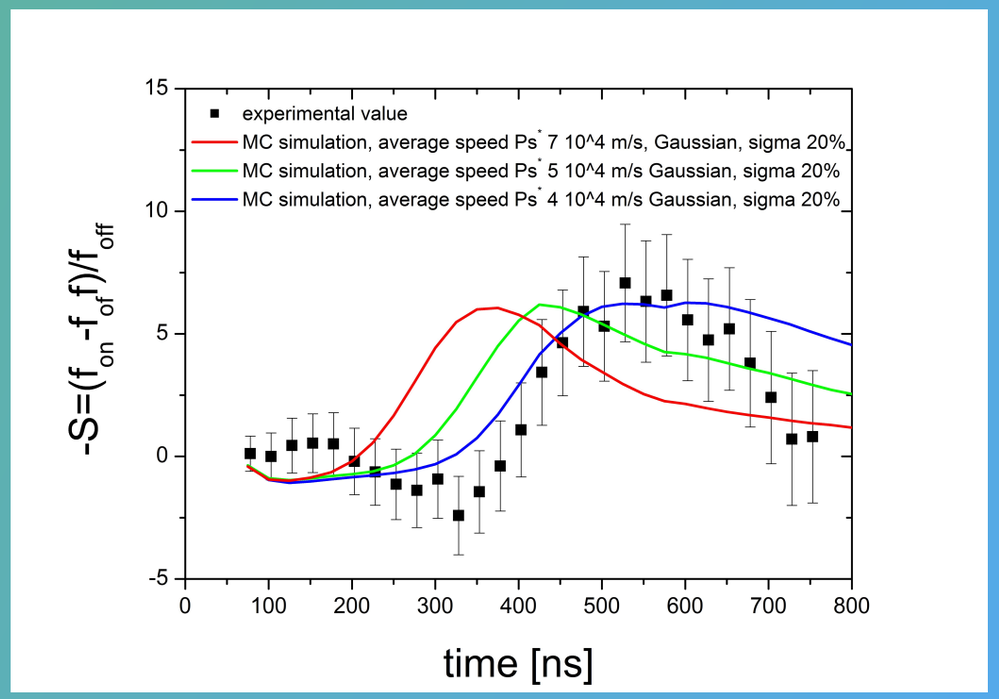
experimental value
MC simulation, average speed Ps* 7 10^4 m/s, Gaussian, sigma 20%
MC simulation, average speed Ps* 5 10^4 m/s Gaussian, sigma 20%
MC simulation, average speed Ps* 4 10^4 m/s Gaussian, sigma 20%
$-S=(f_{on}-f_{of}f)/f_{off}$
15
10
5
0
-5
0
100
200
300
400
500
600
700
800
time [ns]

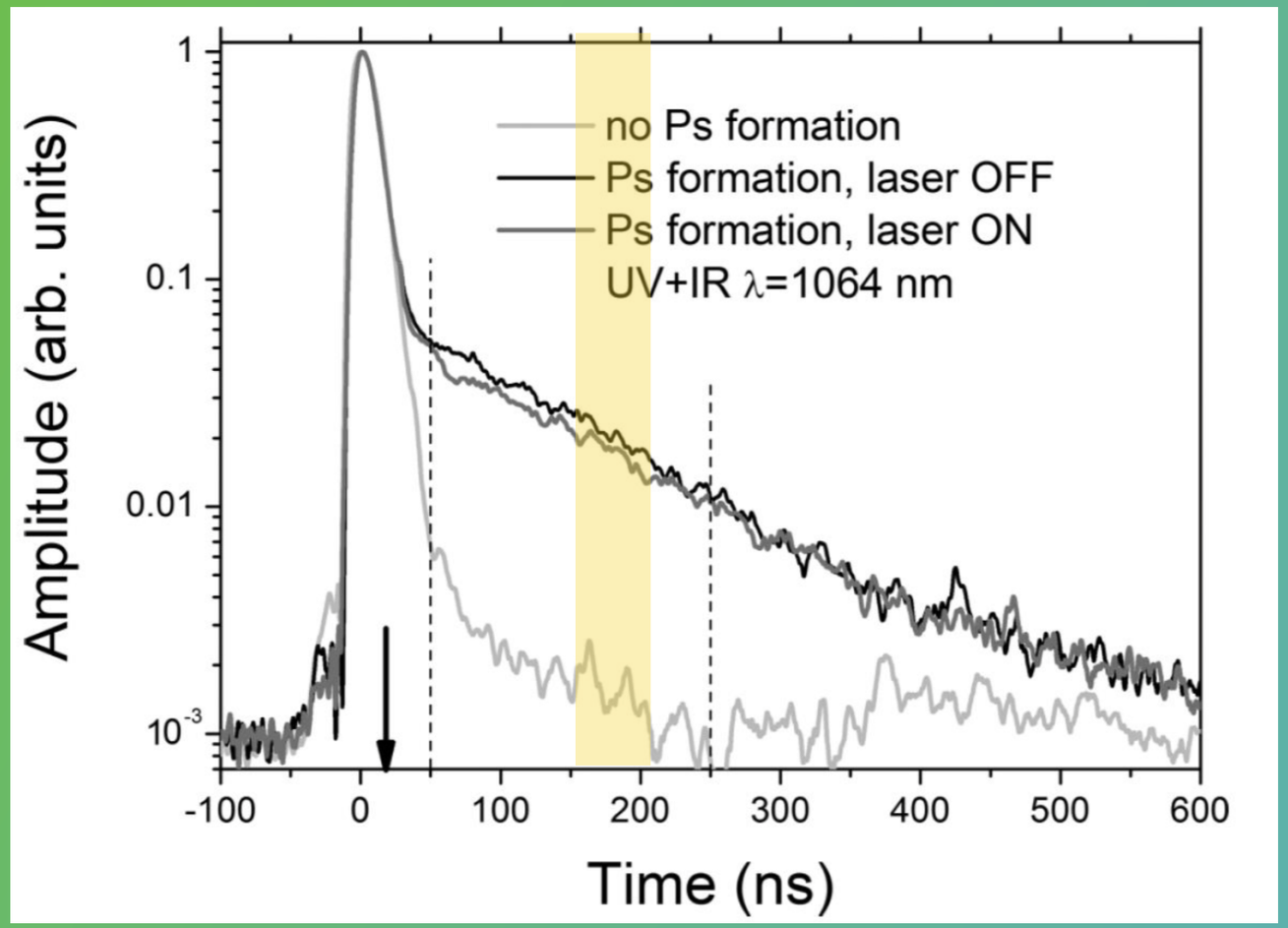
Amplitude (arb. units)
1
0.1
0.01
10^{-3}
no Ps formation
Ps formation, laser OFF
Ps formation, laser ON
UV+IR λ=1064 nm
-100
0
100
200
300
400
500
600
Time (ns)

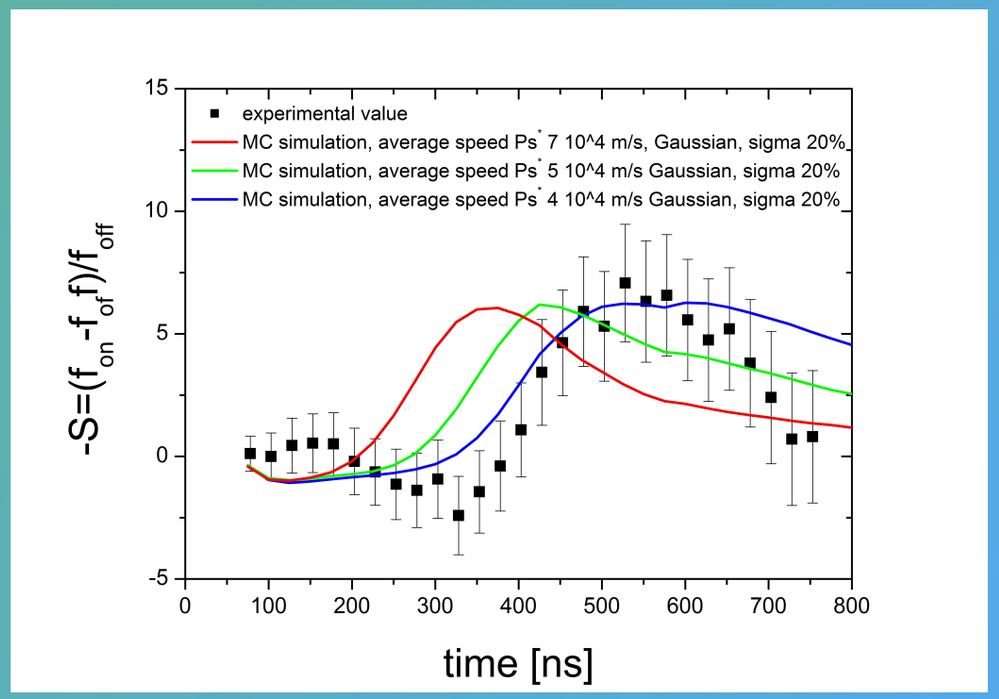
experimental value
MC simulation, average speed Ps* 7 10^4 m/s, Gaussian, sigma 20%
MC simulation, average speed Ps* 5 10^4 m/s Gaussian, sigma 20%
MC simulation, average speed Ps* 4 10^4 m/s Gaussian, sigma 20%
$-S=(f_{on}-f_{of}f)/f_{off}$
15
10
5
0
-5
0
100
200
300
400
500
600
700
800
time [ns]

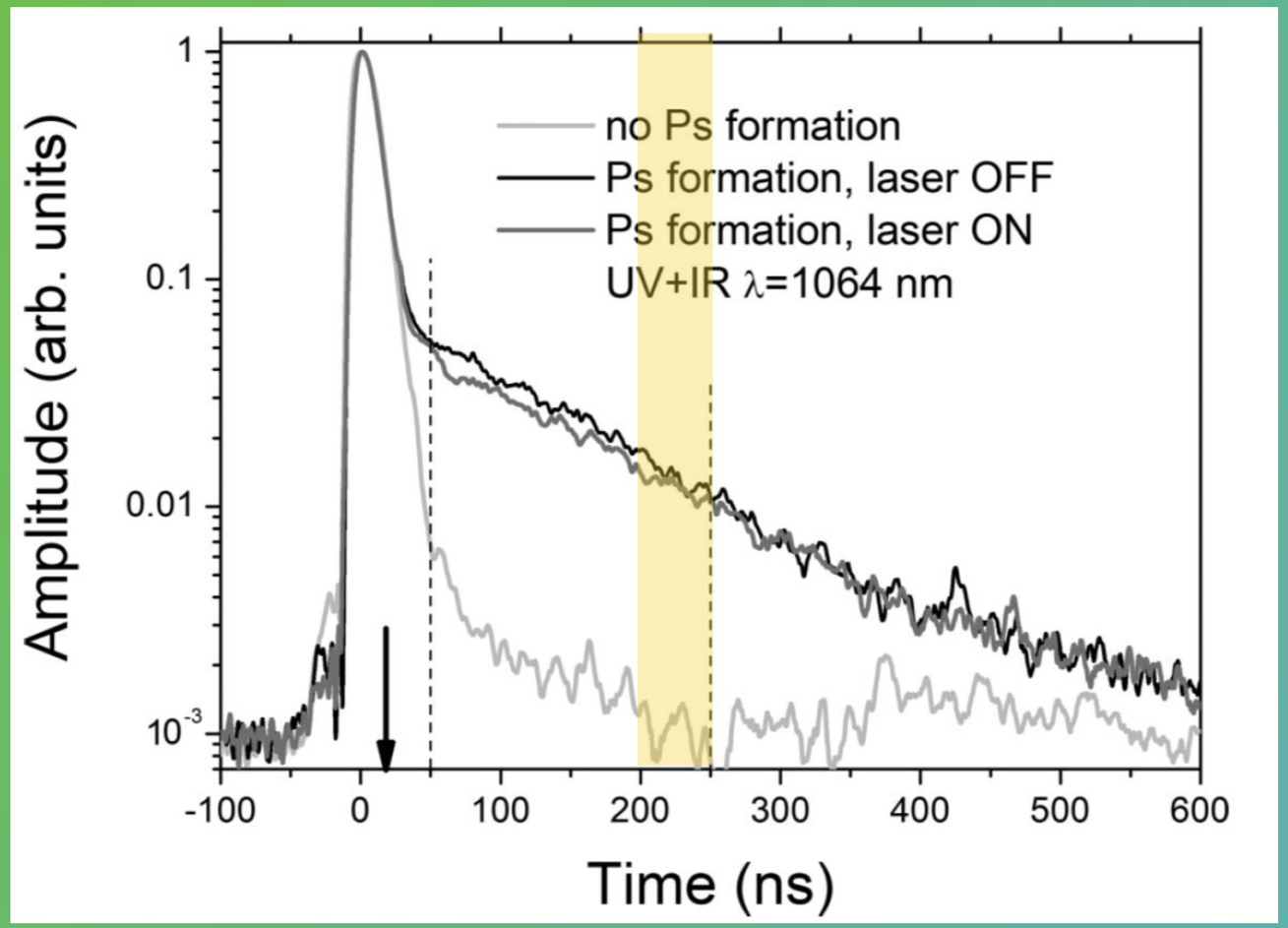
Amplitude (arb. units)
1
0.1
0.01
10^{-3}
no Ps formation
Ps formation, laser OFF
Ps formation, laser ON
UV+IR λ=1064 nm
-100
0
100
200
300
400
500
600
Time (ns)

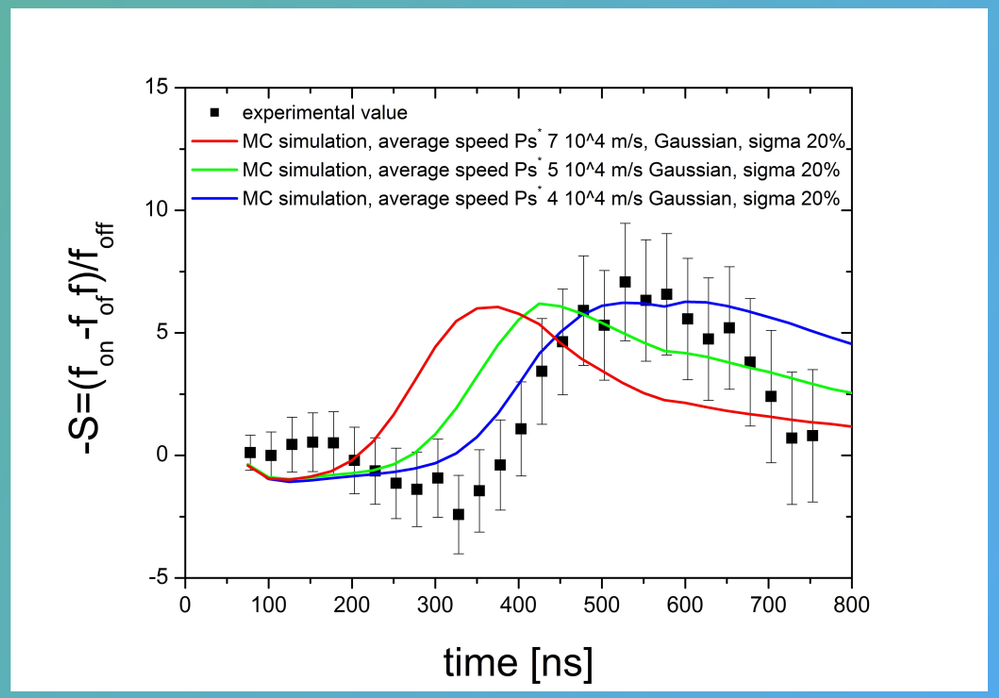
experimental value
MC simulation, average speed Ps* 7 10^4 m/s, Gaussian, sigma 20%
MC simulation, average speed Ps* 5 10^4 m/s Gaussian, sigma 20%
MC simulation, average speed Ps* 4 10^4 m/s Gaussian, sigma 20%
$-S=(f_{on}-f_{of}f)/f_{off}$
15
10
5
0
-5
0
100
200
300
400
500
600
700
800
time [ns]

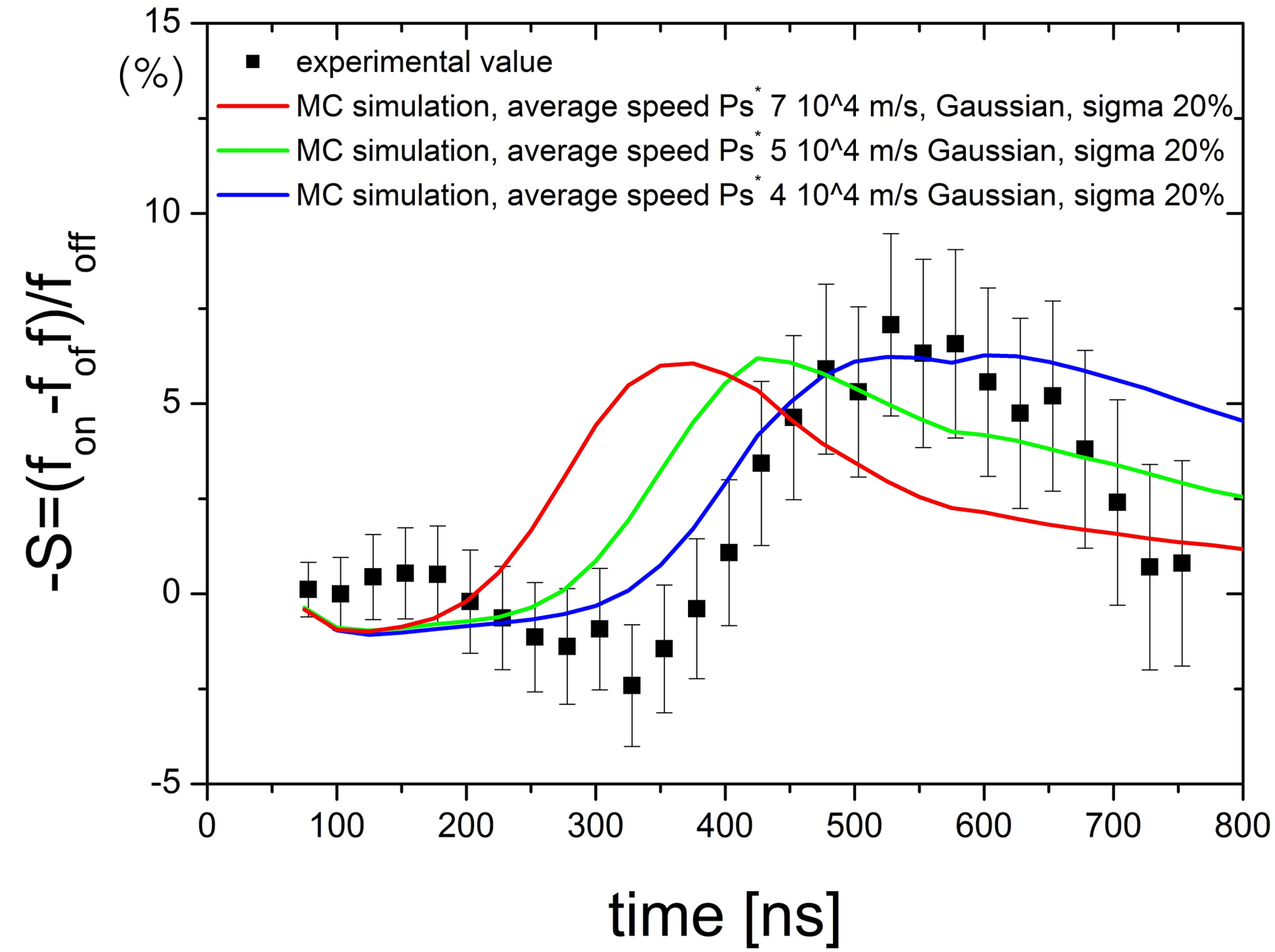
15
(%)
10
5
0
-5
0
100
200
300
400
500
600
700
800
time [ns]
-S=(f_on-f_of f)/f_off
experimental value
MC simulation, average speed Ps* 7 10^4 m/s, Gaussian, sigma 20%
MC simulation, average speed Ps* 5 10^4 m/s Gaussian, sigma 20%
MC simulation, average speed Ps* 4 10^4 m/s Gaussian, sigma 20%

Laser delay has impact on the velocity distribution of Ps*

laser delay= 15 ns

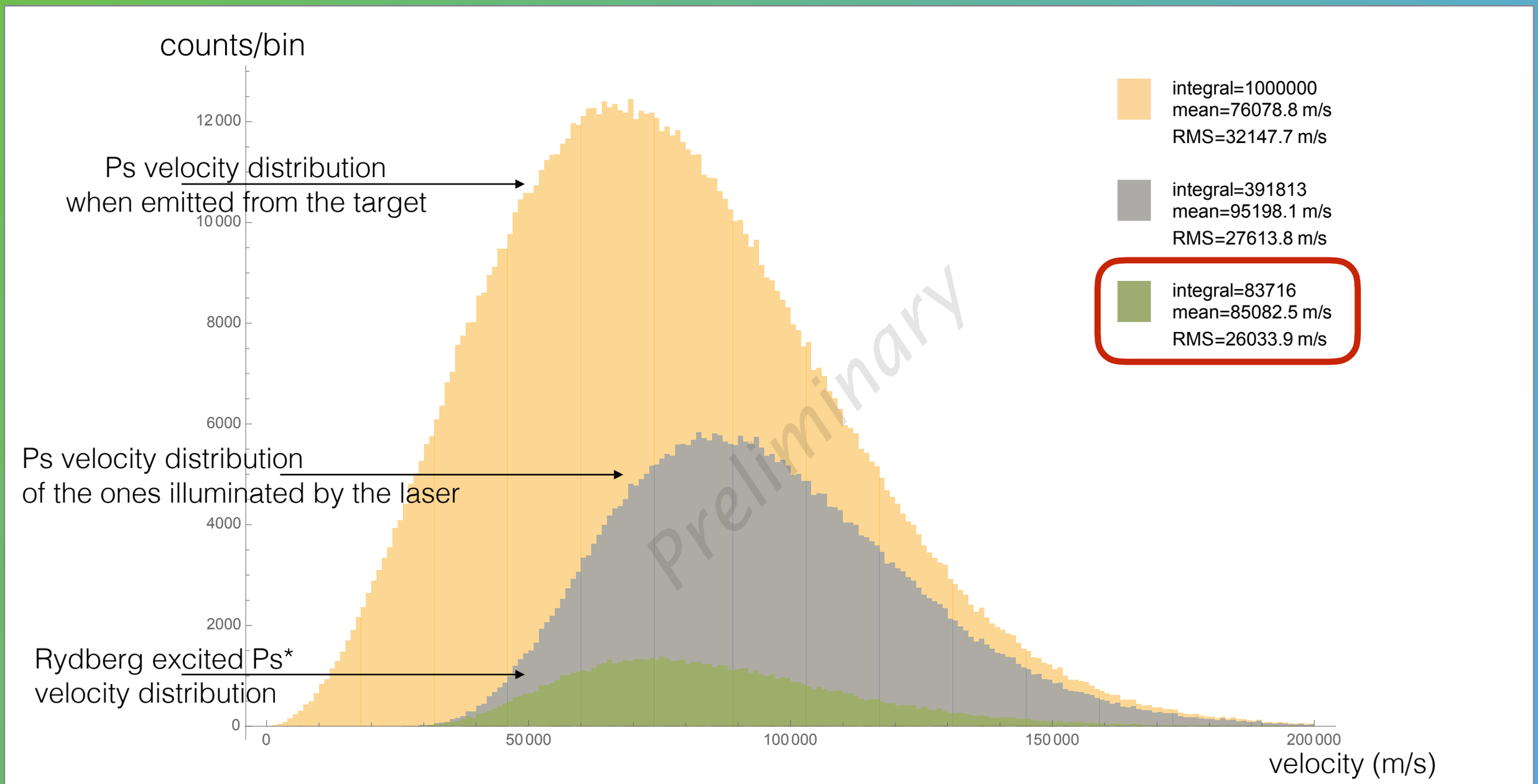

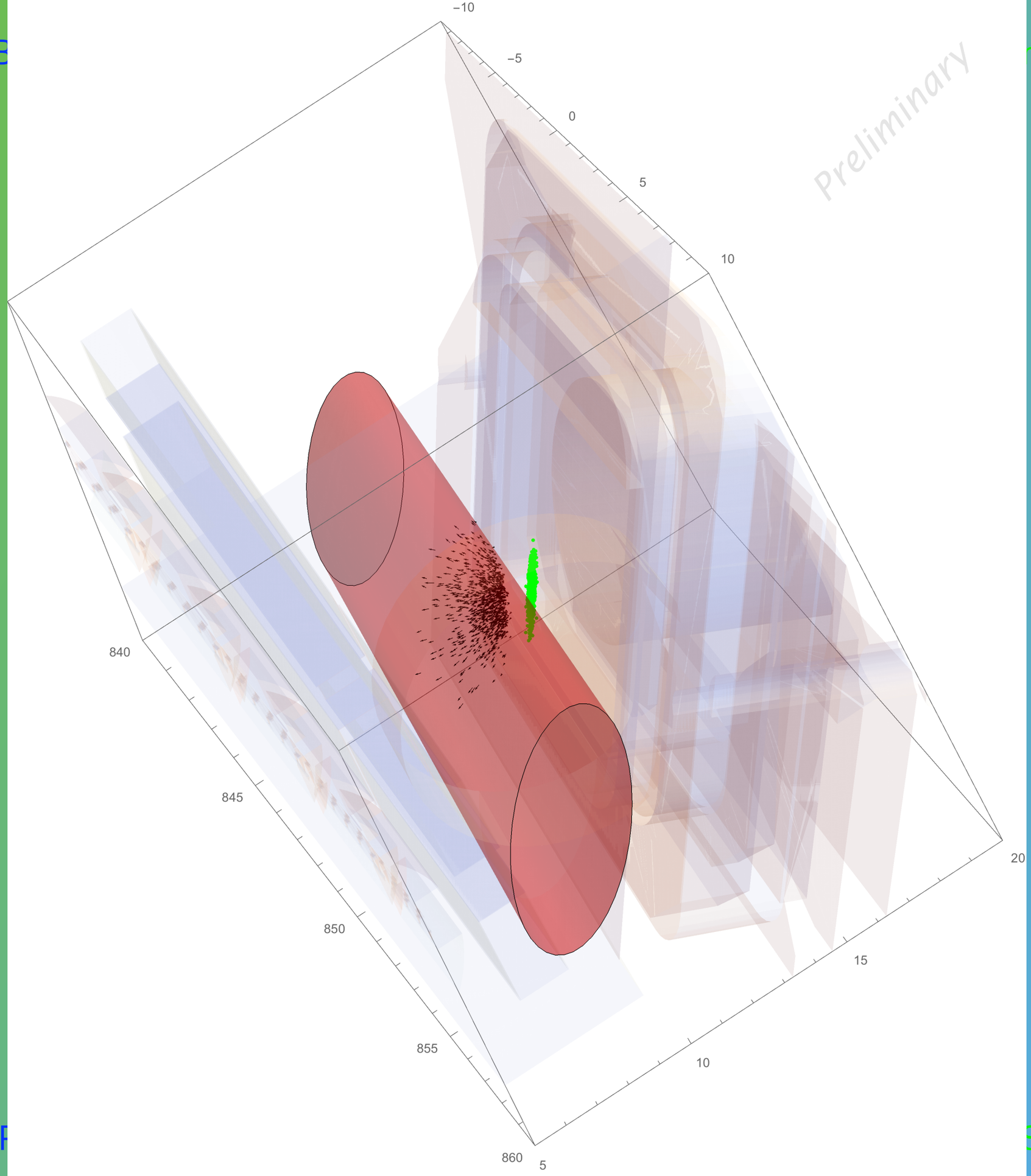
−10
−5
0
5
10
Preliminary
840
845
850
855
860
5
10
15
20

laser delay= 85 ns

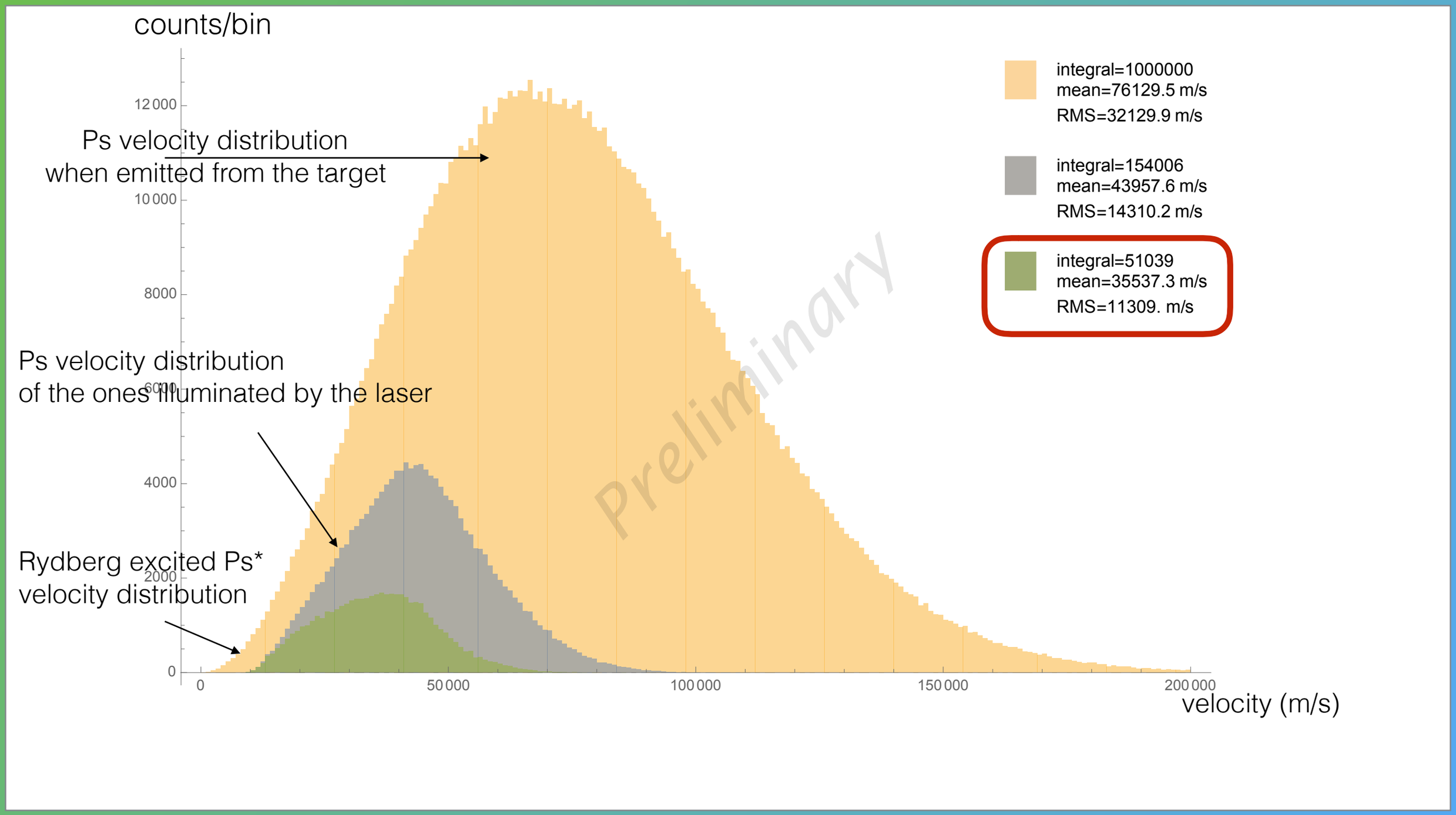

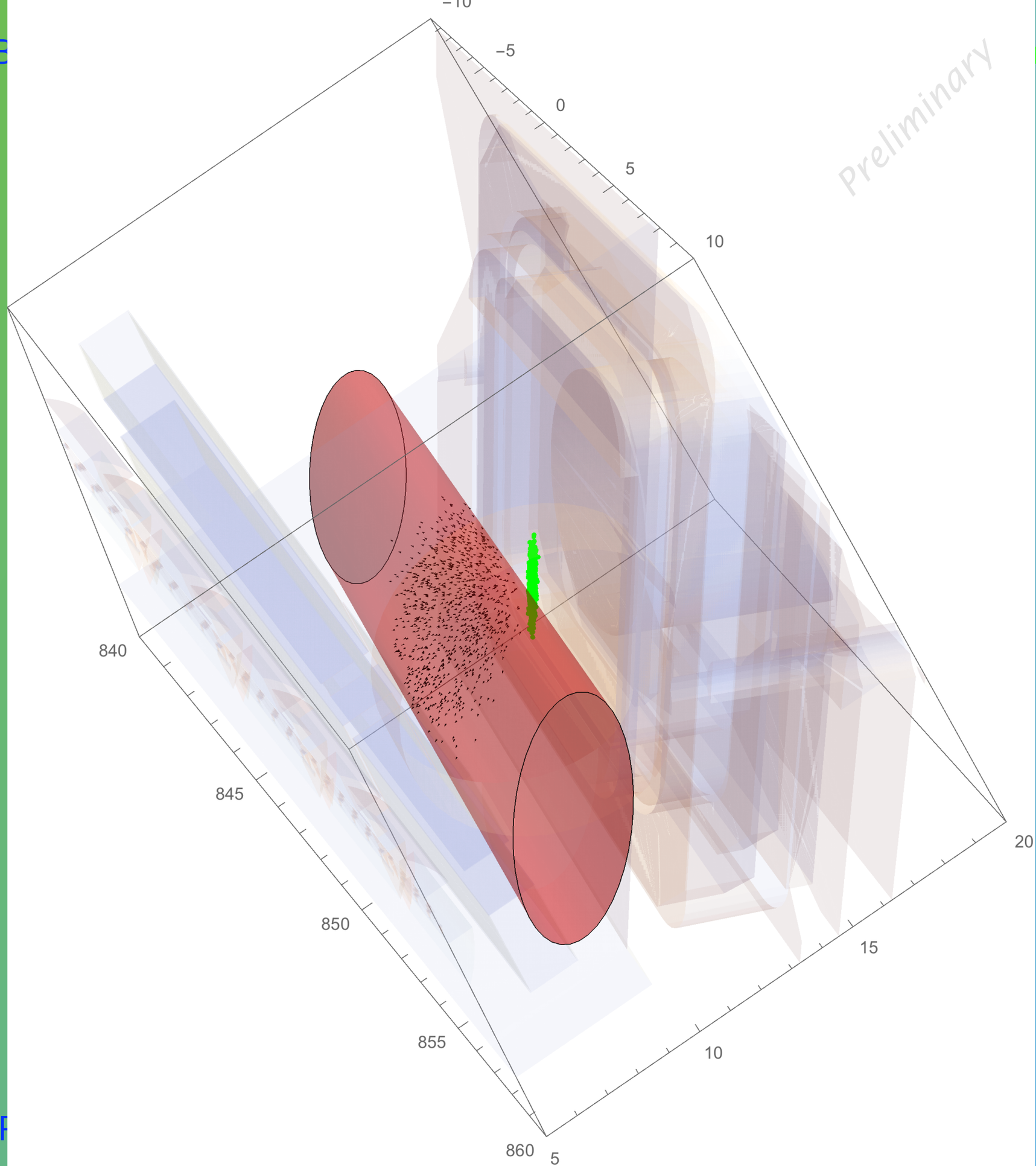
−10
−5
0
5
10
Preliminary
840
845
850
855
860
5
10
15
20

Antihydrogen formation

We are manly interested in Ps* (and in their properties) that can enter the antiproton Penning trap through the mesh and that can reach the antiproton plasma.

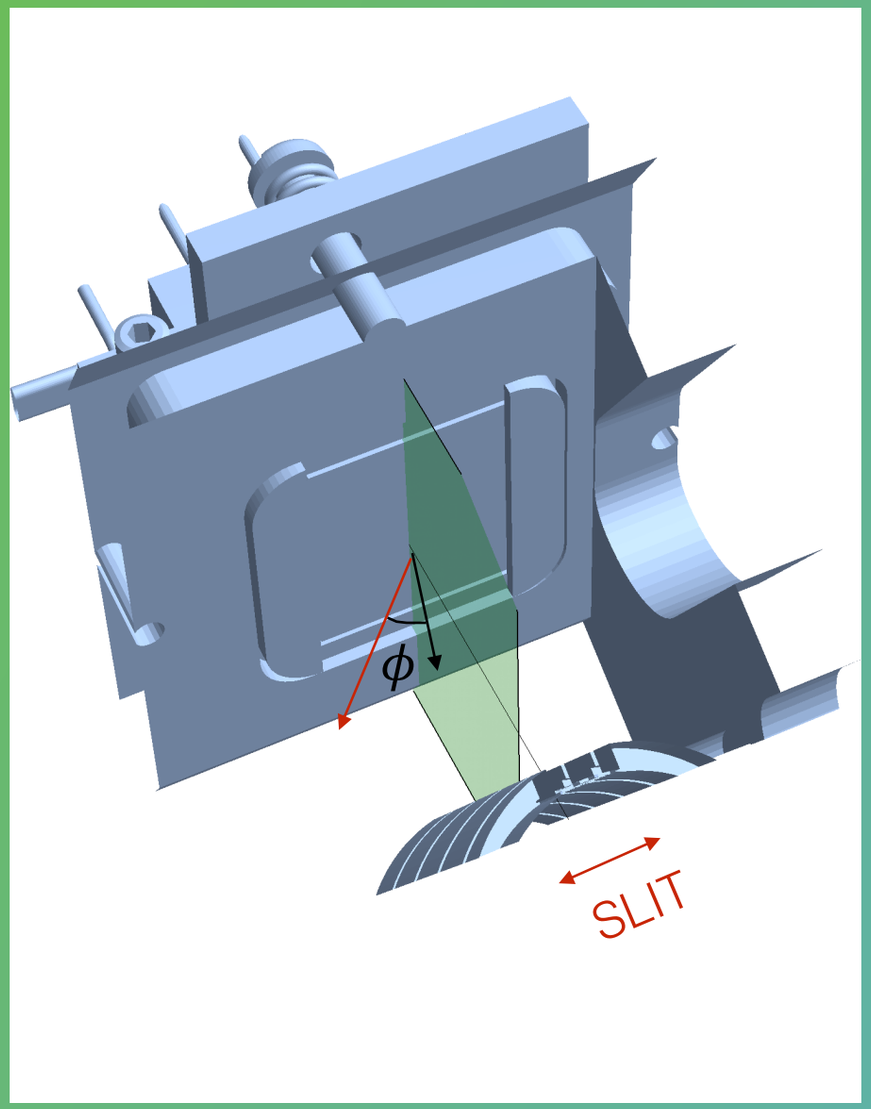

Angular distribution of the Ps/Ps*

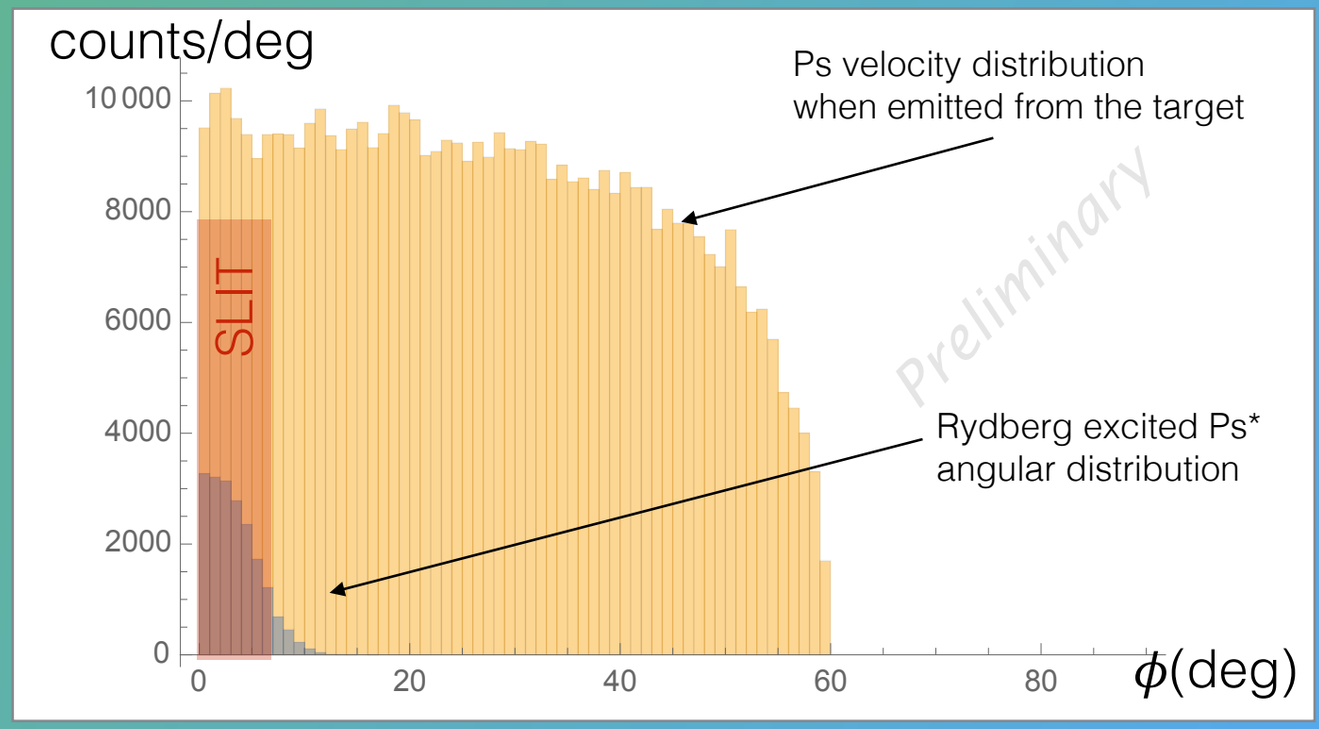

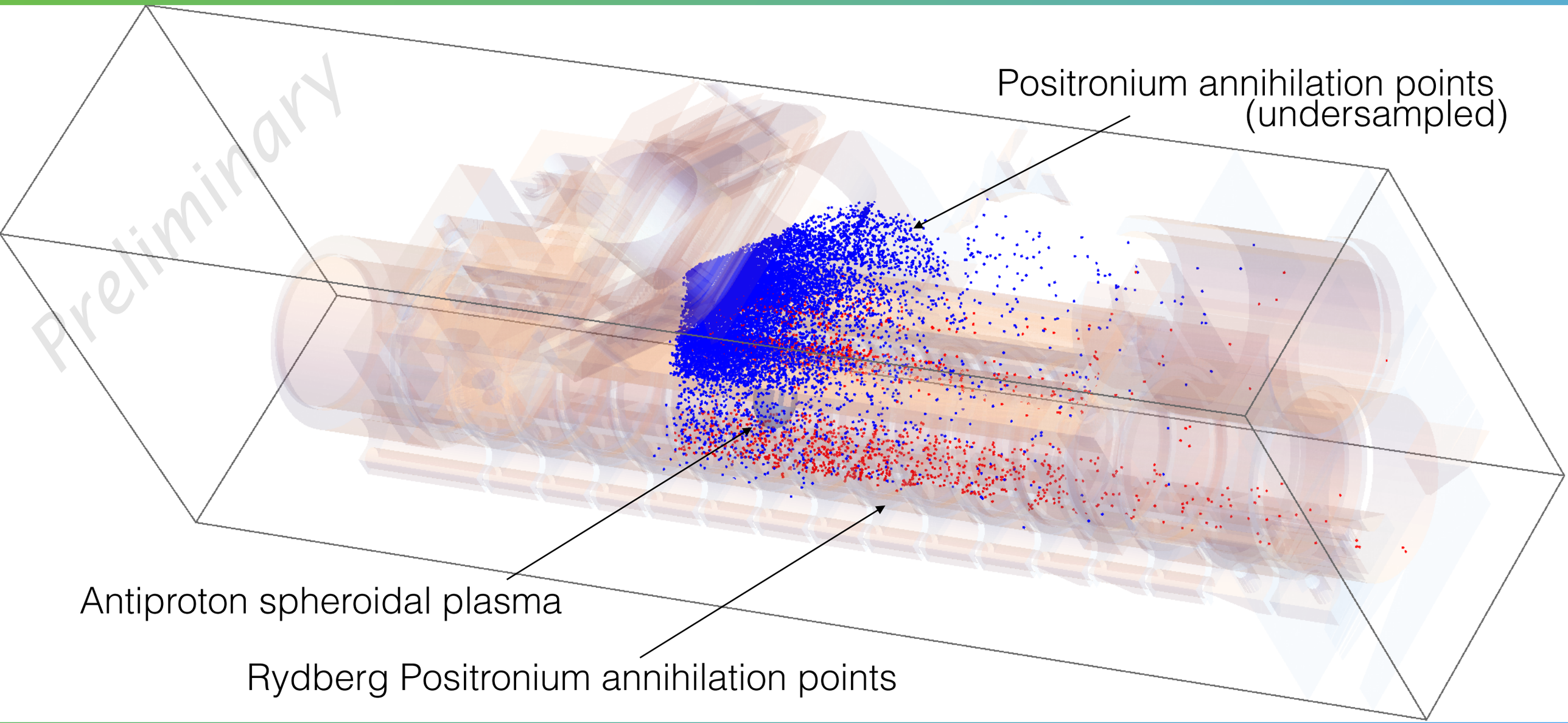
Preliminary
Positronium annihilation points
(undersampled)
Antiproton spheroidal plasma
Rydberg Positronium annihilation points

Antiproton plasma parameters

A charged plasma confined in a Penning trap has been studied in great detail e.g. in:

Daniel H. E. Dubin and T. M. O'Neil
Trapped nonneutral plasmas, liquids, and crystals (the thermal equilibrium states)

Reviews of Modern Physics, Vol. 71, No. 1, January 1999

If we define the Debye length:

$$\lambda_D = \sqrt{\frac{kT}{4\pi n e^2}}$$

The antiprotons cloud is really a plasma when the Debye length is smaller than the cloud side.

If this is true, and if the the equilibrium configuration is reached, the plasma experience a shear-free, rigid rotation flow around the direction of the magnetic field (plus thermal velocity Maxwellian fluctuations) with an angular frequency ω given by:

$$\omega_{\pm} = \frac{\Omega_c \pm \sqrt{\Omega_c^2 - 2\omega_p^2}}{2}.$$

where Ω_c is the cyclotron frequency $\Omega_c = eB/mc$

and ω_p is the plasma frequency $\omega_p = (4\pi n e^2/m)^{1/2}$ $(\omega_p/\Omega_c < 1)$

In general the charge density is given by Poisson's equation for the self-consistent electric potential:

$$4\pi e^2 n = -\nabla^2 e\phi_p$$

where $\phi_P(r,z)$ is the space-charge potential;
Inside the plasma, since the external potential must be shielded out, we have:

$$\phi_p(r,z) + \phi_R(r,z) \simeq \text{const}$$

and $\phi_R(r,z)$ is the effective external potential in the rotating frame:

$$e\phi_R(r,z) = e\phi_T(r,z) + m\omega(\Omega_c - \omega)r^2/2$$

As a consequence, in nearly quadratic potential well ("harmonic well") the plasma shape is a spheroid with a Debye sheath at the plasma edge (whose thickness depends on the plasma temperature)

From the experimental side, we measure the integrated density along the trap axis $\int \rho(r,z)dz$ through a MCP detector coupled to a phosphor screen

S. Aghion et al. (AEGIS COLLABORATION)
"Compression of a mixed antiproton and electron non-neutral plasma to high densities"
Eur. Phys. Journal D, in press

and the total number of antiprotons by external calibrated scintillators.

Number of pbars : ~3,5 x 10^5
Central plasma density: ~9 x 10^6 pbars/cm^3
Plasma size: radius ~2mm, z length ~1 mm
Plasma Temperature : in the ~100 K—1000 K range

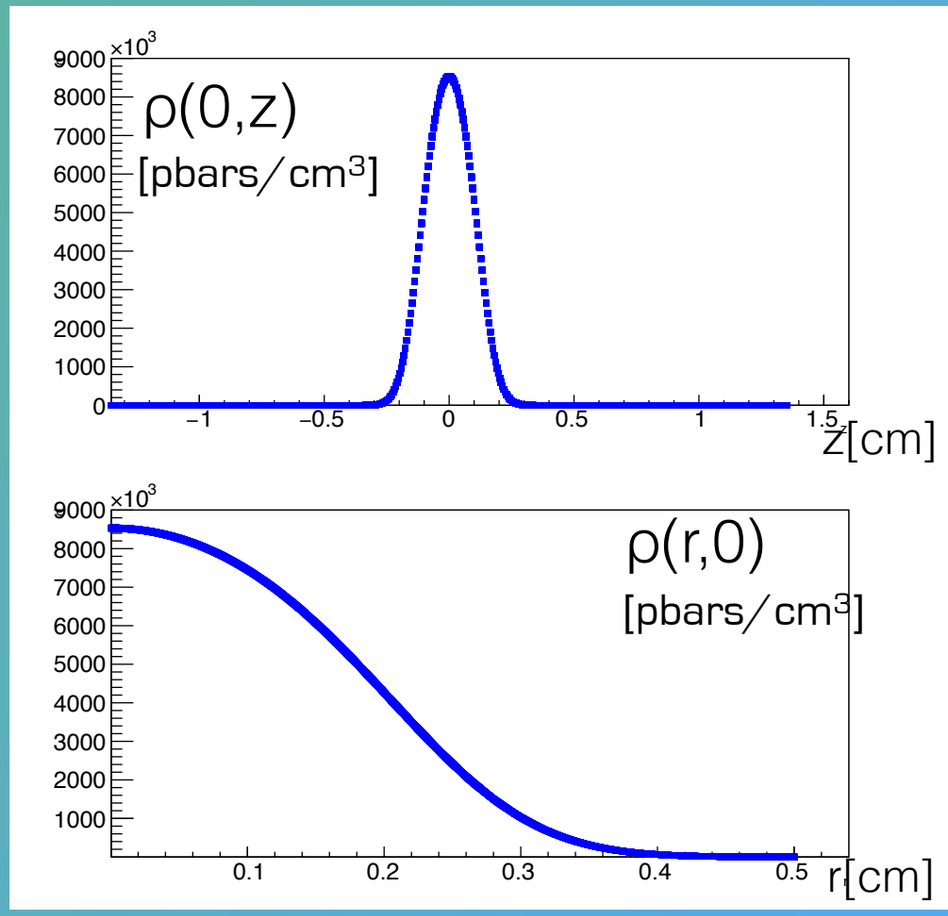

From these data and the analytical model we infer:

Pbar Thermal Velocity: $v_{th} \lesssim 4'000$ m/s

Pbar Rotational Velocity: $v_{rot} \ll 1'000$ m/s

So, the pbar velocity is negligible compared to the Rydberg positronium velocity and we can consider only the latter for the cross section calculations!

Charge Exchange cross section

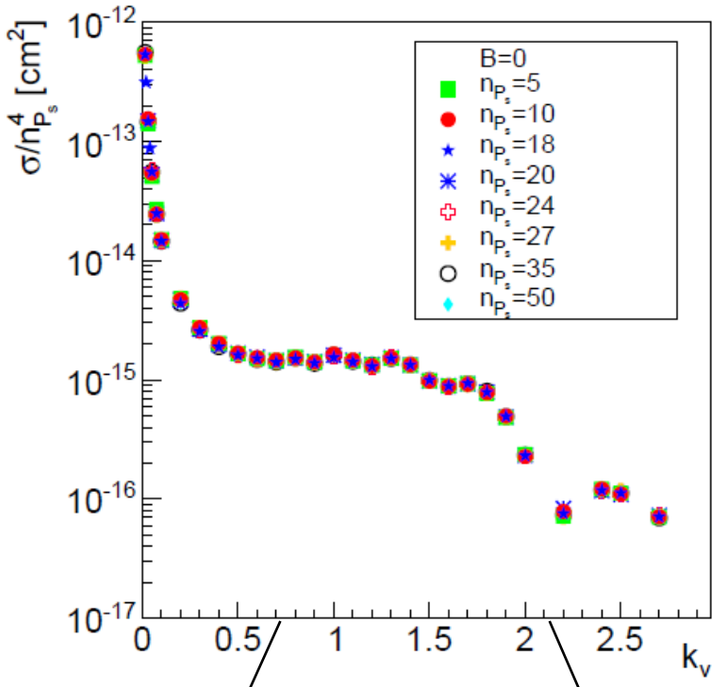

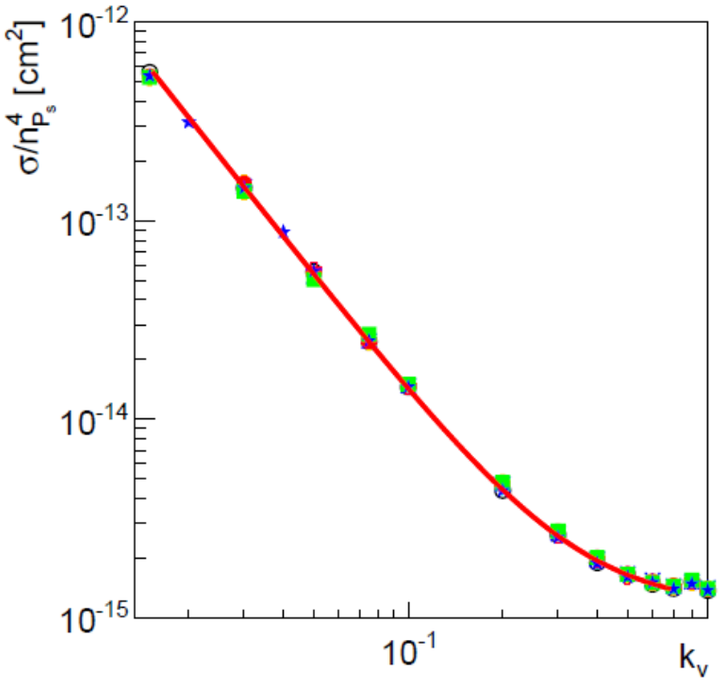

FIG. 2. Charge exchange cross section divided by n_{Ps}^4 (σ/n_{Ps}^4) as a function of k_v with B=0. The results obtained for the various principal quantum number shown in the legend collapse into a universal curve and they cannot be distinguished in the plot. For each n_{P_s} the l_{P_s} and m_{P_s} values are sampled from a canonical ensemble as described in section II. The right plot is a zoom of the region with low k_v values with the fit $\sigma/n_{P_s}^4[cm^2] = \frac{s_1}{k_v^2} + s_2$ superimposed (red line). $s_1 = 1.32 \cdot 10^{-16} cm^2$, $s_2 = 1.12 \cdot 10^{-15} cm^2$.

$$v_{Ps} = 3\ 10^4\, m/s$$

if nPs=17

$$v_{Ps} = 1.2\ 10^5\, m/s$$

if nPs=17

D. Krasnicky, C. Canali,R. Caravita, G. Testera
Phys. Rev. A 94, 022714 (2016)

Classical Calculation

$$\sigma \propto n^4$$

$$\left(v_{cm}^{Ps}\right)_{m/s} = \frac{k_v}{2\, n_{Ps}} 2.19\ 10^6\, m/s$$

A.S. Kadyrov et al.
Nature Comm. 8, 1544 (2017)

Quantum calculation

Classical regime restored if

$$\lambda_{dB} < 2a_0 n_{Ps}^2$$

that is:

$$n_{Ps} k_v > 3.3$$

Plateau regime correct in our range of nPs
Low k_v region and low nPs: σ scales as n^2.....

Equivalent path traveled by Ps* at pbar central density

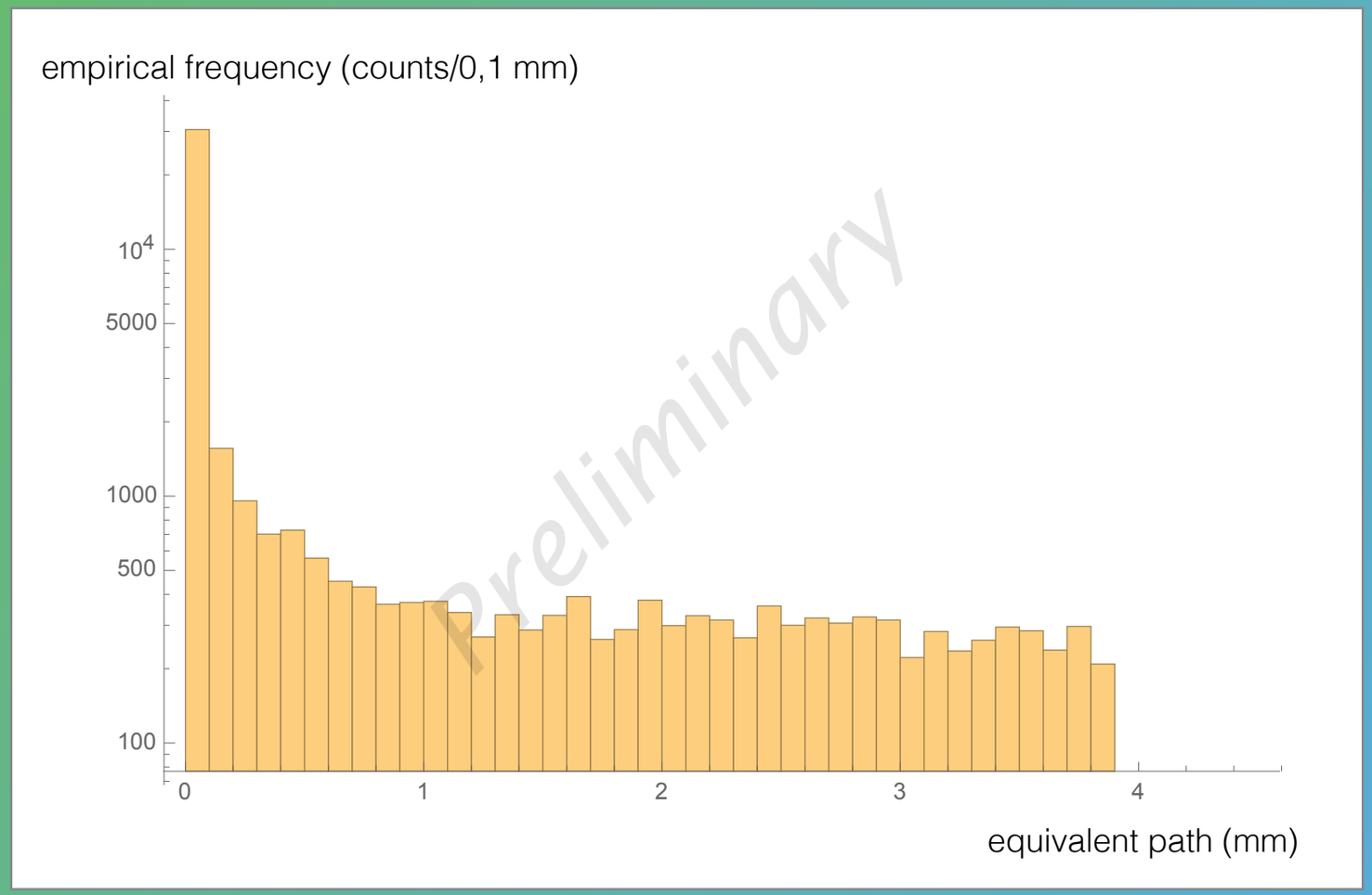

out of 10^6 Ps produced from the target

(laser fired 20 ns after Ps prompt annihilations)

Interaction probability for each Ps* reaching the pbar trap

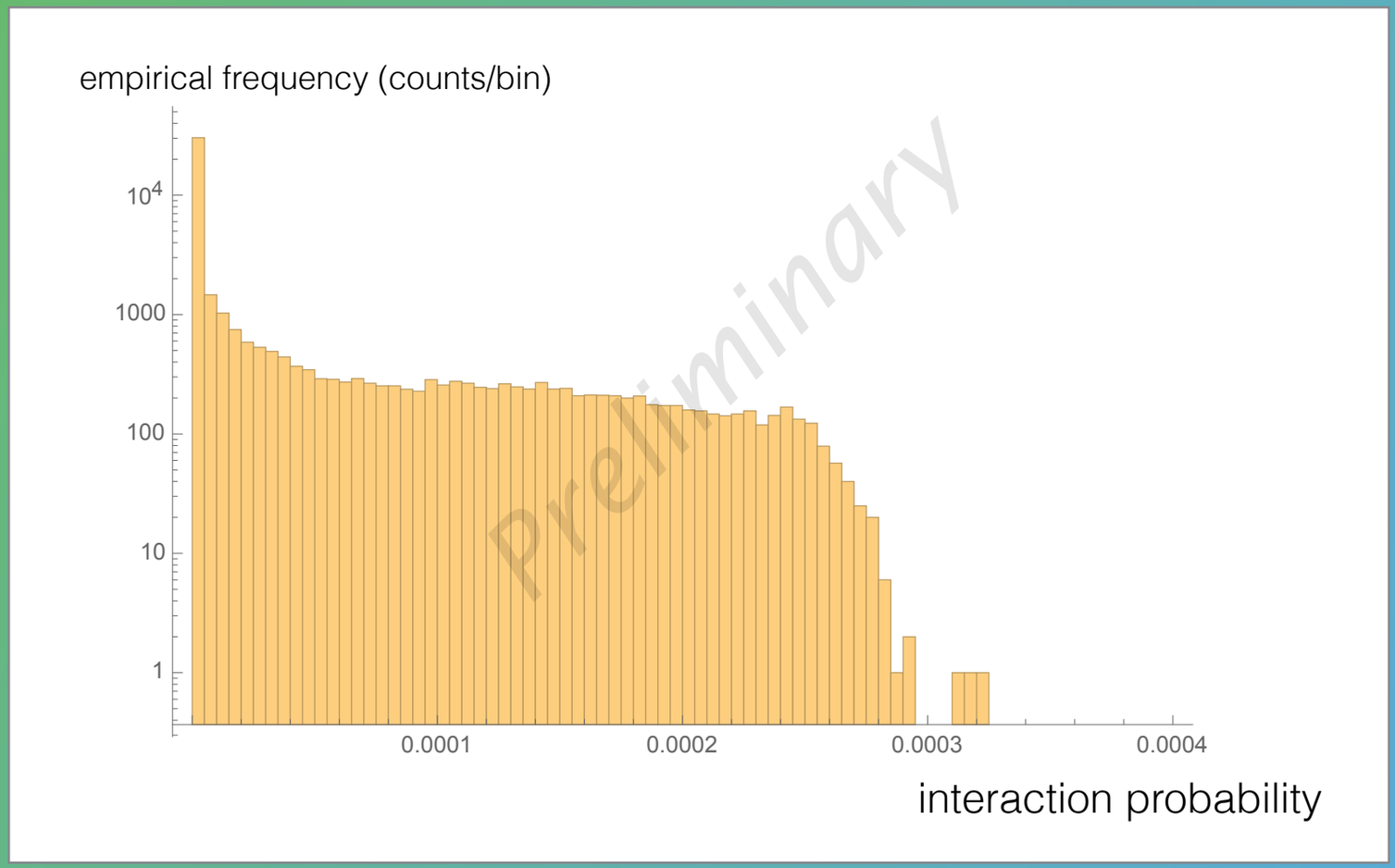

out of 10^6 Ps produced from the target

Rydberg Ps* supposed with n=15

Conclusions

- We have set up a new tool to understand what occurs between the e^+-Ps converter and the trap production region.
- The complexity of the geometry is a serious limit for any kind of Monte Carlo simulation, and we tried to overcome it by splitting the simulation in two parts and keeping the computationally time consuming geometry in the first part.
- Ps laser excitation is modelled in a self-consistent way.
- Charge exchange process is modelled as well.
- A validation of the simulation is underway in a simpler geometry.
- If successful, the Monte Carlo results will be important to optimise the Ps/Ps*/pbar parameters for Hbar production.

Conclusions

- We have set up a new tool to understand what occurs between the e^+-Ps converter and the trap production region.
- The complexity of the geometry is a serious limit for any kind of Monte Carlo simulation, and we tried to overcome it by splitting the simulation in two parts and keeping the computationally time consuming geometry in the first part.
- Ps laser excitation is modelled in a self-consistent way.
- Charge exchange process is modelled as well.
- A validation of the simulation is underway in a simpler geometry.
- If successful, the Monte Carlo results will be important to optimise the Ps/Ps*/pbar parameters for Hbar production.

Thank you for your attention!!!